Journal of Petroleum Science and Engineering 205 (2021) 108773

Contents lists available at ScienceDirect

Journal of Petroleum Science and Engineering

journal homepage: http://www.elsevier.com/locate/petrol

Automated decision support methodology for early planning phase of a multi-reservoir field

I Gusti Agung Gede Angga *, Milan Stanko

Department of Geoscience and Petroleum, Norwegian University of Science and Technology (NTNU), S. P. Andersens veg 15a, 7031, Trondheim, Norway

ARTICLE INFO

Keywords:
Field development planning
Optimization
Proxy model
Mixed-integer linear programming
Uncertainty analysis

ABSTRACT

The field planning process is a crucial phase in the life of a hydrocarbon field when many design features must be decided upon. The field development team has the task of finding a configuration of these field design features which maximizes the value of the company's asset while considering several constraints. This paper presents a decision support methodology suitable for the early stage of the field planning process. The methodology is applied on a synthetic field called Safari. This field is characterized by having multiple reservoir units, where these reservoir units are non-communicating and have distinct properties. The reservoirs, namely Løve, Nesehorn, and Sebra, have original oil-in-place (OOIP) of 75, 55, and 13 million sm^3, respectively. Both Løve and Nesehorn have a permeability of 250 mD, whereas Sebra has a higher permeability of 450 mD. All these reservoirs lie 2500 m below the sea level with an initial reservoir pressure of 280 bara and an initial reservoir temperature of 80 °C. The main part of the methodology is a mathematical optimization that uses (i) proxy models to represent the flow performance of the production system and to estimate the development costs and (ii) piecewise linear (PWL) approximations to represent the non-linear functions. In this study, two optimization problems with the objective function to maximize plateau duration or net present value (NPV) are formulated and solved. The optimization models consider production schedule, drilling schedule, and recovery mechanism as the decision variables. Some constraints concerning production, injection, and drilling are also included in the optimization models. According to the optimization results, the objective value can be improved by considering more decision variables in the optimization problems. For example, including the drilling schedule and recovery mechanism as decision variables gives us 85% higher optimal NPV than optimizing the production schedule alone. Several investigations have been made to reduce the optimization runtime and to ensure the accuracy of the optimization results. Furthermore, the uncertainty of the optimization results has been quantified through uncertainty analyses. These analyses consider three uncertain parameters, i.e., OOIP, development costs, and oil price. Two approaches have been evaluated for conducting the uncertainty analysis, i.e., using the Latin hypercube sampling (LHS) method and using a probability tree. The uncertainty analysis using a probability tree is recommended because it requires less time to complete while produces similar results as the other approach.

1. Introduction

The life cycle of a hydrocarbon field typically consists of the following stages (Jahn et al., 2008; The Ministry of Petroleum and Energy and the Ministry of Labour and Social Affairs, 2018):

1. Business case identification: gaining access, exploration and appraisal
2. Project planning: feasibility studies, conceptual studies and preliminary engineering
3. Project execution: detailed engineering, construction testing and start-up
4. Production
5. Abandonment and decommissioning

The work presented in this paper is relevant for the early phases of field planning, i.e., feasibility studies and conceptual studies. Field planning is a crucial phase in the life of a hydrocarbon field because it aims to determine the *best* strategy to develop the field under significant uncertainties in all aspects, like subsurface, cost, production performance, contractual conditions, among others. The *best* strategy is

* Corresponding author.
E-mail addresses: i.g.a.g.angga@ntnu.no (I.G.A.G. Angga), milan.stanko@ntnu.no (M. Stanko).

https://doi.org/10.1016/j.petrol.2021.108773
Received 13 October 2020; Received in revised form 2 February 2021; Accepted 2 April 2021
Available online 20 April 2021

Abbreviations

ABEX	Abandonment expenditure (unit: Mill. NOK)
AMPL	A mathematical programming language
CAPEX-SUB	Capital expenditure for subsea equipment (unit: Mill. NOK)
CAPEX-TOP	Capital expenditure for topside equipment (unit: Mill. NOK)
CPU	Central processing unit
DRILLEX	Drilling expenditure (unit: Mill. NOK)
EXPEX	Exploration expenditure (unit: Mill. NOK)
FPSO	Floating production storage and offloading
GL	Gas lift
GOR	Gas-oil ratio (unit: sm^3 gas/sm^3 oil)
GPL	General public license
IAM	Integrated asset modeling
ID	Inner diameter (unit: m)
IPR	Inflow performance relationship
IQR	Interquartile range
k_{ro}	Relative permeability of oil
k_{rw}	Relative permeability of water
LHS	Latin hypercube sampling
MBE	Material balance equation
MD	Measured depth (unit: m)
Mill	Million
MILP	Mixed-integer linear programming
MINLP	Mixed-integer non-linear programming
NOK	Norwegian krone
NPD	Norwegian petroleum directorate
NPV	Net present value (unit: Mill. NOK)
OOIP	Original oil-in-place (unit: Mill. sm^3)
OPEX	Operating expense (unit: Mill. NOK)
PI	Productivity index
PWL	Piecewise linear
SOS1	Special ordered sets of type 1
SOS2	Special ordered sets of type 2
TVD	True vertical depth (unit: m)
USD	United State dollar
VRR	Voidage replacement ratio

commonly associated with the technically-feasible strategy that has the highest economic performance.

To fulfill the goal of field planning, a value chain model is typically established by the field development team. In this value chain model, reservoir models are often built and used to determine the reservoirs' time-dependent behavior, such as recovery factor and production profile, for a given set of inputs. The value chain model also includes many field design features that are often considered, such as type of offshore structure, recovery mechanism, number of wells & its drilling schedule, production system layout, production schedule, processing facilities, and many more (Haldorsen, 1996). Decisions on these field design features have impacts not only on the field production profile but also on the cost profile. Thus, they affect the economic of the field development.

The field development team has to configure these field design features such that the economic value of the field is maximized. However, the development team's outcome is often suboptimal. It is because only a few configurations are evaluated due to time constraints. In consequence of this conventional approach, there might be other configurations which might give a higher economic value that are left unstudied. To resolve the problem, optimization can be applied to find, in an automated manner, the best configuration of field design features that fulfills a given set of constraints within a relatively shorter amount of time.

In the literature, there are several studies that involve optimization to assist the field planning process. These studies use optimization to find the best configuration of parameters like well characteristics, drilling program, production and injection strategies, etc., in order to maximize the economic value or the hydrocarbon recovery. Some studies done by Jonsbråten (1998), Tupac et al. (2007), Bellout et al. (2012) and Simonov et al. (2019) use complex reservoir models to represent the reservoir performance. Unfortunately, those complex reservoir models are usually not available in the early of field planning phase. Moreover, these studies only use reservoir models to compute the production profile, neglecting the effect of production network. This simplification may result inaccuracy of the production profile. Other authors such as Nazarian (2002), Litvak et al. (2007), Volz et al. (2008), Litvak and Angert (2009), Litvak et al. (2011), and Silva et al. (2019) have conducted their studies using a more realistic representation of the production system, i.e. by coupling the subsurface models with the production network models. However, even if the field development team managed to built the complex reservoir models at the early of field planning phase and then integrate them with the production network models, performing optimizations on those complex models are challenging tasks because they require considerable computational power. Furthermore, with the use of complex models, we often encounter non-linear optimization problems, which are typically difficult and time-consuming to solve. In addition to the optimization processes, setting up those complex models is often complicated and requires considerable time.

In the field planning process, especially at the early phase, the amount of available information about the field is typically very limited. Moreover, a lot of simplifications are also made when establishing the value chain model. Because of these, the uncertainties of parameters like reservoir characteristics, development/operational costs, oil price, etc., are typically bigger. It is important for the field development team to consider these uncertainties when making decisions on the field design features. Among the studies mentioned earlier, only some of them take into account uncertainties while performing optimization during field planning process. For example, the studies by Litvak et al. (2007), Litvak and Angert (2009) and Litvak et al. (2011) include the subsurface uncertainties, whereas the study by Jonsbråten (1998) considers the uncertainty of oil price.

Recently, González et al. (2019) presented a methodology applicable to the field planning process, particularly for the early stage. The proposed methodology uses optimization to identify the best production strategy for a field. The differentiating features of the methodology are given as follows:

- The methodology involves the development of a proxy model to represent the performance of the production system. The fundamental of the proxy model is the well potential concept that is often used in reservoir engineering. However, the concept has been extended to also include the effect of the production network. The use of this proxy model, instead of a complex numerical model, benefits the optimization process, i.e., reducing the computational power.
- The methodology includes the modeling of an optimization problem to maximize net present value (NPV) subjected to some constraints. The decision variables of the optimization problem are drilling and production schedule. Initially, the optimization problem is modeled as a mixed-integer non-linear programming (MINLP) problem. The authors then reformulated the optimization problem into a mixed-integer linear programming (MILP) problem by approximating the non-linearities with piecewise linear (PWL) functions, using the

SOS2 model. The advantages of having an MILP problem when compared against the non-linear optimization problem are (i) it usually requires less computational effort to solve, (ii) it guarantees the global optimal solutions, and (iii) the existing algorithms to solve the problem are relatively mature.
- The methodology evaluates the effect of several uncertain parameters -such as costs, reservoir size, well productivity, and layout of the production system- by using a probability tree.

This paper presents a further development of the automated field planning methodology proposed by González et al. (2019). The distinctive characteristics and contributions of the present study are given as follows:

- The study applies and extends the methodology for a field with three reservoir units. In addition to drilling and production schedule, the recovery mechanism of each reservoir unit is considered for optimization. Additionally, injection volumes constrains were included depending on the injectors' drilling schedule. These require fundamental and major changes in the optimization model presented by González et al. (2019).
- The study develops an optimization model to maximize field plateau duration.
- The study explores ways to speed up the optimization process, e.g., (i) determining proper numbers of breakpoints for constructing the PWL functions, (ii) identifying the more-efficient and rigorous approach to compute the production and injection rates of gas and water, (iii) testing different solvers. Moreover, to ensure the accuracy of the optimization results, the study evaluates (i) different breakpoints selection methods and (ii) different numerical integration techniques for estimating the cumulative production/injection.
- The study compares two methods for quantifying the effect of uncertainties on the optimization results, i.e., by using the Latin hypercube sampling (LHS) method and by using a probability tree. The uncertainty analysis performed in the study considers three uncertain parameters, i.e., original oil-in-place (OOIP), development costs, and oil price.

Like the methodology proposed by González et al. (2019), this study also uses a proxy model representing the flow performance of the production system. The proxy model is obtained by simulating an integrated model of the production system. The integrated model couples reservoir models, well models, and a production network model. There are some simplifications made for constructing the integrated model, namely:

1. The reservoir is modeled with the tank model.
   In the early phases of field planning, we typically have very little knowledge about the reservoir. Maps showing the distribution of reservoir properties, such as porosity and permeability, are not yet available. Thus, it is common to model the reservoir as a tank with homogeneous properties. Using the material balance equation (MBE) on the tank model, we may predict the reservoir performance.
2. The producers in each reservoir are identical.
   Due to the absence of properties distribution maps, it is frequent to represent all producers penetrating a single reservoir unit with a single well model. One important input for constructing the well model is permeability, which will be used to estimate the well's productivity index (PI). The input permeability is usually acquired from the well-testing interpretation or the core analysis.
3. The future inflow performance relationship (IPR) of the producers was corrected with the variation in oil, gas, and water saturation of the reservoir tank.
   For constructing the well model, we employ a reservoir inflow model that takes permeability and relative permeability curve as the inputs. In this inflow model, the fluid saturation of the reservoir tank influences the well's future PI and therefore affects the well's future IPR.
4. For simulations of scenarios with pressure support, we assume that the injection process has a voidage replacement ratio (VRR) of 100%. VRR of 100% means that the volume of fluid injected into a reservoir tank is equal to the volume of fluid produced from that reservoir tank. One implication of the assumption is that the injection process starts as the reservoir begins to produce.

These simplifications are the most significant limitations of the integrated model.

2. Methodology

This section briefly describes the main workflow followed in the study (see Fig. 1). At first, two proxy models are developed. One proxy model is to represent the production system's flow performance, while the other one is to estimate the development and operational cost (discussed in Section 3). Using the proxy models, the next step is to formulate production optimization problems. Two optimization problems are modeled in this study. One aims to maximize plateau duration (discussed in Section 4) and the other one aims to maximize NPV (discussed in Section 5). The presence of some non-linear functions in the formulations makes the optimization problems categorized as MINLP problems. Next, we transform the MINLP problems into MILP problems by approximating the non-linearities with piecewise linear (PWL) functions, and then we solve those MILP problems (discussed in Section 6). The final part of the study is to quantify the effects of uncertainties on the optimization results (discussed in Section 9).

3. Description of the Safari field case and the proxy models

The work presented in this paper is based on a synthetic case named Safari. The Safari field is an imaginary offshore field located in the North Sea, east of Johan Sverdrup and Grane field and west of Haugesund. The field is characterized by having multiple reservoir units that are non communicating and have unique properties. The field consists of three undersaturated oil reservoirs, i.e. Løve, Nesehorn, and Sebra. Løve is characterized by nearly circular reservoir shape, highest oil-in-place, and heavier oil. Nesehorn and Sebra are almost identical in term of reservoir properties, except Sebra has much less oil-in-place but has higher permeability. All production wells are completed with gas-lift as the artificial lift method. Development using an FPSO is chosen for the field. In this development alternative, production from each reservoir is tied with a separate flowline to a constant-pressure separator at the FPSO. Moreover, the facilities construction and installation phase is commenced from 1st January 2019 and lasts for four years. The field first

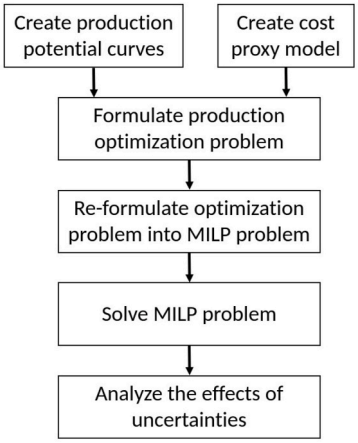

Fig. 1. Main workflow of the study.

oil and abandonment are expected to be in 2023 and 2040, respectively, which gives a total production period of 17 years. This production period was considered constant during the optimization. More details about the Safari field are given in Appendix A.

Production potential curves are generated as a proxy model to represent the flow performance of the production system considering reservoir unit, well and gathering network. As the reservoir units are hydraulically independent from each other, their production potential curves were generated independently. These curves indicate the maximum oil production rate as a function of cumulative oil production, reservoir unit, recovery mechanism and number of producers. These production potential curves allow us to plan a production schedule without a need to run a simulation of the production system model (González et al., 2019; Angga, 2019). Further discussion about production potential curves is provided by Stanko (2020).

The workflow for generating the production potential curves is depicted in Fig. 2. First, the reservoir models and the well models are established. The reservoir models are created using a commercial material balance simulator (MBAL), whereas the well models are constructed using a commercial steady-state well simulator (PROSPER). Next, a production network model is built using a commercial steady-state network simulator (GAP). In this software, the reservoir models and the well models are coupled with the production network model to form an integrated model of the production system.

A production potential curve is obtained by running one simulation of the integrated model. The number of simulation cases required depends on the number of combinations of (i) reservoir unit, (ii) recovery mechanism, and (iii) number of producers. In this study, 80 simulation cases are defined and stored in a case database in Excel. After defining the simulation cases, we combine the case database and the integrated model of the production system using a commercial Integrated Asset Modeling (IAM) software called RESOLVE. The use of the IAM software allows us to run the simulation cases automatically. All the aforementioned commercial programs are provided by Petroleum Experts (2020).

After the simulation cases are defined and the integrated model is built, the production potential curves are generated by running simulations ensuring that maximum oil rate is produced at each time. This usually requires opening wellhead chokes fully, performing gas-lift allocation optimization, and often discarding production constraints (e.g., erosional velocity, maximum liquid rate, maximum gas rate). The runtime to complete one simulation ranges from 15 min to 3 h, depending on the complexity of the integrated production system model. After performing the simulations, the production potential curves are finally constructed by plotting the maximum oil production rate against the cumulative oil production. Examples of the production potential curve are provided in Appendix B.

In this study, an optimization problem to maximize NPV is formulated and solved. To enable us calculating the NPV, another proxy model to estimate the development and operational cost is developed based on input data provided by AkerSolutions. In this proxy model, the development and operational cost comprised of six elements, i.e., exploration expenditure (EXPEX), drilling expenditure (DRILLEX), abandonment expenditure (ABEX), capital expenditure for subsea equipment (CAPEX-SUB), capital expenditure for topside equipment (CAPEX-TOP), and operating expense (OPEX). For each element, the cost associated is expressed as a linear equation with single or multiple explanatory variables. Furthermore, the costs amounts are paid on specific years. Details of the cost proxy model are given in Appendix C.

4. Optimization model to maximize field plateau duration ("CASE-1")

Mathematical formulation of an optimization problem with the objective function to maximize plateau duration is discussed in this section. In this optimization model, the variables to optimize comprise (i) the yearly production and injection rates, (ii) number of wells and their drilling schedule and (iii) recovery mechanism for every reservoir unit.

The objective function deployed on the optimization model is expressed as follows:

$$\text{minimize} \quad \sum_{t\in\{2,\ldots,n_t\}} \left(q_{o,f}^{plateau} - q_{o,f}^{t}\right) \tag{1}$$

where $q_{o,f}^{plateau}$: a desired plateau rate for the field oil production, $q_{o,f}^{t}$: field oil production rate at time t. The time scale used in this work is years. Visually, the objective function is aimed to minimize the gray area in Fig. 3.

The optimization is subjected to several equality and inequality constraints. The first constraint is that the yearly field oil rates must be lower than or equal to the desired plateau rate.

$$q_{o,f}^{t} \le q_{o,f}^{plateau}, \quad \forall t \in \{2,\ldots,n_t\} \tag{2}$$

Oil production rate of a particular reservoir is restrained by the

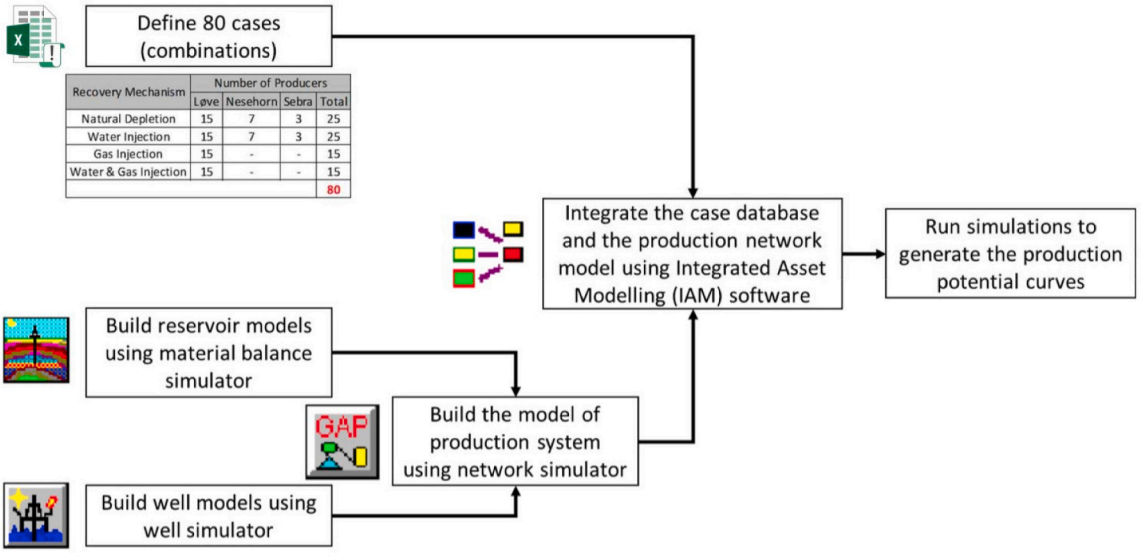

Fig. 2. Workflow for generating the production potential curves.

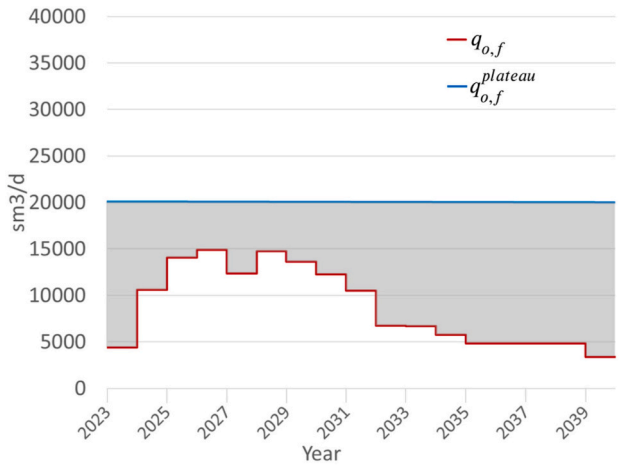

Fig. 3. Visualization of the objective function, i.e., to minimize the gray area. The blue line is the desired plateau rate for field oil production and the red line is the actual field oil production rate. (For interpretation of the references to colour in this figure legend, the reader is referred to the Web version of this article.)

maximum rate the reservoir can deliver, which is represented by the production potential.

$$q_{o,r}^{t} \le q_{opp,r}^{t}, \quad \forall r \in R \quad \text{and} \quad \forall t \in \{2,\ldots,n_t\} \tag{3}$$

$$q_{o,r}^{t} \le q_{opp,r}^{t-1}, \quad \forall r \in R \quad \text{and} \quad \forall t \in \{2,\ldots,n_t\} \tag{4}$$

where $q_{o,r}^{t}$ and $q_{opp,r}^{t}$ are the oil production rate and the oil production potential of reservoir r at time t, respectively. As mentioned earlier, the oil production potential of reservoir r at time t is partly dependent on the cumulative oil production of that reservoir at time t. In this work, the cumulative oil production is estimated with the backward rectangular integration rule. With this integration technique, the oil production rate $q_{o,r}^{t}$ is assumed to be constant from time $t-1$ to t. For this reason, a constraint expressed by Eq. (4) is included in the formulation.

For a particular time, the oil production potential of a reservoir is non-linearly dependent on (i) the reservoir, r, (ii) the recovery mechanism of the reservoir, M_r, (iii) the number of oil producers in the reservoir at that time, $N_{op,r}^{t}$ and (iv) the cumulative oil produced from the reservoir by that time, $N_{p,r}^{t}$.

$$q_{opp,r}^{t} = q_{opp}\left(r, M_r, N_{op,r}^{t}, N_{p,r}^{t}\right) \tag{5}$$

In this work, four types of recovery mechanism are considered, i.e., natural depletion ($M_r = 1$), water injection ($M_r = 2$), gas injection ($M_r = 3$) and water-gas injection ($M_r = 4$).

As mentioned earlier, the injection process is assumed to have a VRR of 100%. One consequence of this assumption is that the injection process begins from the first day of the production period. Another consequence is that the injection rate can be very high in order to balance the production rate. To achieve a very high injection rate, a very high injection pressure might be needed. An enormous injection pressure could damage the formation around the injector. To prevent this from happening, we introduce operational constraints that limit the injection rate.

$$q_{gi,r}^{t} \le N_{gi,r}^{t-1} \cdot q_{gi}^{capability}, \quad \forall r \in R \quad \text{and} \quad \forall t \in \{2,\ldots,n_t\} \tag{6}$$

$$q_{wi,r}^{t} \le N_{wi,r}^{t-1} \cdot q_{wi}^{capability}, \quad \forall r \in R \quad \text{and} \quad \forall t \in \{2,\ldots,n_t\} \tag{7}$$

where $q_{gi,r}^{t}$: gas injection rate of reservoir r at time t, $q_{wi,r}^{t}$: water injection rate of reservoir r at time t, $N_{gi,r}^{t-1}$: number of gas injectors in reservoir r at time $t-1$, $N_{wi,r}^{t-1}$: number of water injectors in reservoir r at time $t-1$, $q_{gi}^{capability}$: maximum gas injection rate for each gas injector, $q_{wi}^{capability}$: maximum water injection rate for each water injector. By applying these constraints in the optimization model, the production rate is indirectly restrained so that the injection rate does not exceed its upper limit. In addition, the constraints might keep the injection pressure not becoming extremely high.

The rate of gas injected to reservoir r at time t is computed using the following linear function.

$$q_{gi,r}^{t} = q_{gi}\left(G_{i,r}^{t-1}, G_{i,r}^{t}\right) \tag{8}$$

where $G_{i,r}^{t-1}$ and $G_{i,r}^{t}$ are the cumulative gas injection to reservoir r at time $t-1$ and time t, respectively. The cumulative gas injection itself is a non-linear function of (i) the reservoir, (ii) the recovery mechanism of the reservoir and (iii) the cumulative oil produced from the reservoir.

$$G_{i,r}^{t} = G_i\left(r, M_r, N_{p,r}^{t}\right) \tag{9}$$

The same approach is taken to compute the water injection rate, $q_{wi,r}^{t}$, the gas production rate, $q_{g,r}^{t}$, and the water production rate, $q_{w,r}^{t}$.

Several constraints related to drilling are included in the optimization model. For example, the number of wells is non-decreasing from time to time. This means that once the well is drilled, it will not be plugged and abandoned until the end of the field lifetime.

$$N_{op,r}^{t-1} \le N_{op,r}^{t}, \quad \forall r \in R \quad \text{and} \quad \forall t \in \{2,\ldots,n_t\} \tag{10}$$

$$N_{gi,r}^{t-1} \le N_{gi,r}^{t}, \quad \forall r \in R \quad \text{and} \quad \forall t \in \{2,\ldots,n_t\} \tag{11}$$

$$N_{wi,r}^{t-1} \le N_{wi,r}^{t}, \quad \forall r \in R \quad \text{and} \quad \forall t \in \{2,\ldots,n_t\} \tag{12}$$

where $N_{op,r}^{t}$, $N_{gi,r}^{t}$ and $N_{wi,r}^{t}$ are the numbers of oil producers, gas injectors and water injectors, respectively, available in reservoir r at time t.

The numbers of injectors have to satisfy the following constraints.

$$N_{gi,r}^{t} \le z_{gi,r} \cdot N_{gi,r}^{max}, \quad \forall r \in R \quad \text{and} \quad \forall t \in T \tag{13}$$

$$N_{wi,r}^{t} \le z_{wi,r} \cdot N_{wi,r}^{max}, \quad \forall r \in R \quad \text{and} \quad \forall t \in T \tag{14}$$

where $N_{gi,r}^{max}$ and $N_{wi,r}^{max}$ are the maximum numbers of gas injectors and water injectors, respectively, allowed to be drilled in reservoir r. In equations above, $z_{gi,r}$ and $z_{wi,r}$ are binary variables where the values depend on the recovery mechanism of reservoir r. $z_{gi,r}$ becomes one if the reservoir applies gas injection or water-gas injection ($M_r = 3$ or $M_r = 4$), and becomes zero if the reservoir chooses natural depletion or water injection ($M_r = 1$ or $M_r = 2$). For $z_{wi,r}$, it becomes one if the reservoir applies water injection or water-gas injection ($M_r = 2$ or $M_r = 4$), and becomes zero if the reservoir chooses natural depletion or gas injection ($M_r = 1$ or $M_r = 3$).

In addition, the following constraints are included to govern the number of pre-drilled production and injection wells and the number of wells drilled per year.

$$N_{op,f}^{1} \le N_{op}^{pre-drilled} \tag{15}$$

$$N_{gi,f}^{1} + N_{wi,f}^{1} \le N_{it}^{pre-drilled} \tag{16}$$

$$N_{wt,f}^{t} - N_{wt,f}^{t-1} \le N_{wt}^{max-drilled}, \quad \forall t \in \{2,\ldots,n_t\} \tag{17}$$

where $N_{op}^{pre-drilled}$: the maximum number of pre-drilled oil producers, $N_{it}^{pre-drilled}$: the maximum number of pre-drilled injectors, $N_{wt,f}^{t}$: the number of all wells (producers and injectors) in the field at time t, $N_{wt}^{max-drilled}$: the maximum number of wells drilled per year.

5. Optimization model to maximize NPV ("CASE-2")

This section discusses the formulation of another optimization problem. The optimization model has the objective to maximize NPV by configuring the same decision variables as in the previous optimization model. The objective function is expressed as follows:

$$\text{maximize} \quad NPV \tag{18}$$

The reference date for NPV calculation is 1st Jan 2019. In addition, taxes and royalties are not considered for NPV calculation.

All constraints included in the previous optimization model are applied for this formulation, except the one related to the desired plateau rate (Eq. (2)). In addition to that, several other parameters and variables required for NPV calculation are included in this formulation. For example, the present value of EXPEX, $P_{v,ex}$, is modeled with a constant.

$$P_{v,ex} = constant \tag{19}$$

In the cost proxy model, DRILLEX is solely dependent on the number of wells drilled. Therefore, the present value of DRILLEX for pre-drilled wells, $P_{v,dx}^{pre-drilled}$, only depends on the number of pre-drilled wells, $N_{wt,f}^{1}$,

$$P_{v,dx}^{pre-drilled} = P_{v,dx}\left(N_{wt,f}^{1}\right) \tag{20}$$

while the present value of DRILLEX made at time t, $P_{v,dx}^{t}$, only depends on the number of wells drilled from time t to $t+1$.

$$P_{v,dx}^{t} = P_{v,dx}\left(N_{wt,f}^{t+1}, N_{wt,f}^{t}\right) \tag{21}$$

The present value of ABEX, $P_{v,ax}$, depends on the numbers of oil producers, gas injectors and water injectors at the end of the field lifetime, i.e., time $t = n_t$.

$$P_{v,ax} = P_{v,ax}\left(N_{op,f}^{n_t}, N_{gi,f}^{n_t}, N_{wi,f}^{n_t}\right) \tag{22}$$

In the cost proxy model, CAPEX-SUB has linear dependency on the numbers of subsea templates, $N_{st,f}$, and subsea xmas trees, $N_{xt,f}$.

$$P_{v,sx} = P_{v,sx}\left(N_{st,f}, N_{xt,f}\right) \tag{23}$$

The subsea templates which have four available slots are allocated for the oil producers. On the contrary, the subsea xmas trees are intended for the gas or water injectors. The numbers of subsea templates and xmas trees are obtained by applying the following constraints.

$$N_{st,f} = \sum_{r \in R} N_{st,r} \tag{24}$$

$$N_{st,r} \geq \frac{N_{op,r}^{n_t}}{4} \tag{25}$$

$$N_{xt,f} = N_{gi,f}^{n_t} + N_{wi,f}^{n_t} \tag{26}$$

where $N_{st,r}$: the number of subsea templates in reservoir r, $N_{op,r}^{n_t}$: the number of oil producers in reservoir r at the end of the field lifetime.

The present value of CAPEX-TOP, $P_{v,tx}$, is determined based on the production capacities of the processing facility, i.e., $q_o^{capacity}$, $q_g^{capacity}$ and $q_w^{capacity}$.

$$P_{v,tx} = P_{v,tx}\left(q_o^{capacity}, q_g^{capacity}, q_w^{capacity}\right) \tag{27}$$

The production capacities of the processing facility are obtained by applying the following constraint.

$$q_l^{capacity} \geq q_{l,f}^{t}, \quad \forall l \in \{o, g, w\} \quad \text{and} \quad \forall t \in \{2, \ldots, n_t\} \tag{28}$$

The present values of all expenditures made before the field enters the production period, i.e., before 1st Jan 2023, are summarized in a variable called $P_{v,pp}$. The value of the variable is computed with the following expression.

$$P_{v,pp} = P_{v,ex} + P_{v,dx}^{pre-drilled} + P_{v,ax} + P_{v,sx} + P_{v,tx} \tag{29}$$

With reference to the operating costs proxy model, the present value of OPEX spent at time t, $P_{v,ox}^{t}$, is a linear function of (i) the number of oil producers available for maintenance and (ii) the average production rates of oil, gas and water from time $t-1$ to t.

$$P_{v,ox}^{t} = P_{v,ox}\left(N_{op,f}^{t-1}, q_{o,f}^{t}, q_{g,f}^{t}, q_{w,f}^{t}\right) \tag{30}$$

In this optimization model, the source of revenue is limited only to the sales of oil production. The present value of revenue obtained at time t, $P_{v,re}^{t}$, depends on (i) the amount of oil produced from time $t-1$ to t, (ii) the oil price, P_o, and (iii) the exchange rate, X_r. Both oil price and exchange rate are inputs for the optimization, and they are assumed constant throughout the life of the field.

$$P_{v,re}^{t} = P_{v,re}\left(N_{p,f}^{t}, N_{p,f}^{t-1}, P_o, X_r\right) \tag{31}$$

The discounted values of the cash flow of various points in time are computed based on the present values of DRILLEX, OPEX and revenue.

$$D_{cf}^{t} = D_{cf}\left(P_{v,dx}^{t}, P_{v,ox}^{t}, P_{v,re}^{t}\right) \tag{32}$$

NPV is finally determined using the following equation.

$$NPV = -P_{v,pp} + \sum_{t \in T} D_{cf}^{t} \tag{33}$$

6. Linear reformulation and solving the optimization problems

The presence of some non-linear functions in the previous formulations makes the optimization problems fall in a class called mixed-integer non-linear programming (MINLP) problem. Due to the irregular behavior of the non-linear function, some challenges emerge when solving an MINLP, such as difficulty to verify the global optimal and high optimization runtime. Therefore, the optimization problem has been reformulated as a mixed-integer linear programming (MILP) problem. To do so, each of the non-linear functions is replaced with a piecewise linear (PWL) function. The PWL functions are obtained by imposing SOS2 or SOS1 constraints. SOS2 is an ordered set of non-negative variables, which at most two can be non-zero, and if two are non-zero these must be consecutive in their ordering. On the other hand, SOS1 ensures only one variable can be non-zero in an ordered set of non-negative variables. A more detailed explanation about PWL approximation is available in the following literature: Codas et al. (2012); Silva and Camponogara (2014); Hoffmann (2014); Hoffmann and Stanko (2017); Hoffmann et al. (2019); Angga (2019). Detailed MILP formulations for both optimization problems are provided in Appendix E and F.

To solve the MILP problems, we use commercial solvers such as CPLEX (IBM, 2020) and Gurobi (GUROBI OPTIMIZATION, 2020). These commercial solvers implement and combine the simplex algorithm and the branch-and-cut algorithm. A more detailed explanation about the simplex algorithm and the branch-and-cut algorithm can be found in Dantzig (1951, 1963); Crowder et al. (1983); Hoffman and Padberg (1991); Grötschel and Holland (1991); Padberg and Rinaldi (1991). In this work, formulations of the optimization problems are scripted in a modeling language named AMPL (A Mathematical Programming Language). AMPL is designed to solve a wide range of optimization problems, and it closely resembles the symbolic algebraic notation that many modelers use to describe mathematical programs (AMPL, 2020). This makes it convenient to formulate and solve an optimization problem in AMPL. In addition, AMPL offers an interface to various commercial solvers for solving many classes of mathematical optimization.

7. Optimization results

In this section, we show the benefit of involving more decision variables for optimization. Previously, we have formulated two optimization problems, one to maximize field plateau duration and another one to maximize NPV, by changing the production schedule, drilling schedule, and recovery mechanism. We called these optimization problems CASE-1 and CASE-2, respectively. In addition, two other optimization problems have been formulated and solved in this work, i.e., REF-CASE-1 and REF-CASE-2. These optimization problems have the same objective functions as CASE-1 and CASE-2, except they only optimize the production schedule. For the REF cases, the recovery mechanism and drilling schedule input were defined manually by engineers and deemed as the most appropriate. Table 1 shows the differences between the optimization models. Inputs for the drilling schedule and the recovery mechanism are specified by the user. To produce comparable results, the criteria for specifying the input drilling schedule are similar to the drilling constraints applied in the optimization models, i.e., Eq. (10) to Eq. (17). These constraints specify (i) that once the wells are drilled it is not possible to "undrill" them, (ii) that the total number and type of injection wells depend on the recovery mechanism, and (iii) that there is a maximum number of wells allowed to drill each year.

The objective value, optimality gap and runtime for each optimization model are summarized in Table 2. The time to solve REF-CASE-1 and REF-CASE-2 is minimal. The values of the optimality gap for these optimization models indicate that the global optimal solutions have been found. On the other hands, the optimization routines for CASE-1 and CASE-2 are stopped once the runtime reaches the specified time limit, i.e., 12 h. The values of the optimality gap for these optimization models indicate that there might exist a better feasible solution which could improve the current-best objective value. However, even though the best integer solutions for CASE-1 and CASE-2 are not guaranteed to be the global optimal solutions, CASE-1 has a better objective value than REF-CASE-1, while CASE-2 has a much better objective value than REF-CASE-2 ($\approx$ 85% higher NPV). Based on these findings, it can be concluded that involving more decision variables in the optimization model could further improve the objective value, but consequently requires a longer optimization runtime.

Other optimization results like recovery mechanism, drilling schedule and production schedule are provided in Appendix G. In general, the optimization results suggest:

- To apply water-gas injection for Løve and water injection for Nesehorn and Sebra as their recovery mechanism
- Not to drill and produce the reservoir units in sequence, but better to develop them simultaneously
- It is not necessary to drill new wells in the mid-to-late field lifetime because the field production is already limited by some operational constraints, e.g. the processing capacity of produced water.

Table 1
Summary of optimization models.

	CASE-1	REF-CASE-1	CASE-2	REF-CASE-2
Objective function	max plateau duration	max plateau duration	max NPV	max NPV
Production schedule (q^t_o, q^t_g, q^t_w, q^t_{gi}, q^t_{wi})	variable	variable	variable	variable
Drilling schedule (N^t_{op}, N^t_{gi}, N^t_{wi})	variable	input	variable	input
Recovery mechanism (M)	variable	input	variable	input

Table 2
Optimization results.

	CASE-1	REF-CASE-1	CASE-2	REF-CASE-2
Objective value	190421 sm3/d	201293 sm3/d	32068 mill. NOK	17387 mill. NOK
Optimality gap	1.53%	0.00%	16.88%	0.00%
Runtime	12 h.	0.23 s.	12 h.	0.13 s.
Number of variables	8113	3814	8197	3898
Number of constraints	2488	1986	2603	2101

8. Improving the computational efficiency and accuracy

The way we formulate an optimization problem often has an impact on the optimization runtime. This section investigates several approaches to lower the optimization runtime while maintaining a good degree of accuracy of the optimization results. The findings of these investigations have been implemented to the formulations presented previously.

8.1. Determining the appropriate numbers of breakpoints for constructing the PWL functions

For constructing a PWL function, we need to define a set of breakpoints which will be used for making the linear interpolation. The more breakpoints involved, the better the PWL function represents the non-linear behavior of the original function. However, more breakpoints involved also mean more variables in the optimization problem, and thus lead to a longer optimization runtime. Therefore, there is a balance to find between the optimization runtime and the accuracy of the PWL approximation.

An investigation was carried out to find the required numbers of breakpoints, particularly the N_p breakpoints for making PWL approximations of several non-linear functions. This investigation uses the simpler optimization problem, i.e., the REF-CASE-1. Seven cases with different number of N_p breakpoints are tested (as shown in Table 3). In this investigation, the N_p breakpoints are selected with a constant interval depending on the number of N_p breakpoints used (for example, see Fig. 4). Note that the N_p breakpoints defined for a particular case are used for constructing all the production potential curves.

CASE-3 is REF-CASE-1 with the highest number of N_p breakpoints (30). Since this case uses more N_p breakpoints than the other tested cases, the results obtained from this case are considered as the most accurate results and therefore defined as the references for comparison. To have a quantitative comparison, the relative error, E_r, is calculated. This relative error indicates how far the results of a particular case deviate from the results of the reference case. The expression to compute E_r is given as follows:

Table 3
Comparison of cases evaluated for determining the appropriate number of N_p breakpoints.

CASE nr.	Number of N_p breakpoints	Maximum E_r (reference = CASE-3)				Meet below 10% criteria?
		Løve	Nesehorn	Sebra	Field	
3	30	0.00%	0.00%	0.00%	0.00%	Yes
4	25	0.46%	6.61%	0.98%	3.19%	Yes
5	20	0.62%	2.07%	6.30%	1.12%	Yes
6	15	0.67%	3.24%	2.60%	1.60%	Yes
7	10	1.19%	3.96%	7.13%	2.51%	Yes
8	7	3.69%	4.65%	*12.93%*	3.69%	*No*
9	5	8.30%	9.18%	*19.27%*	8.30%	*No*

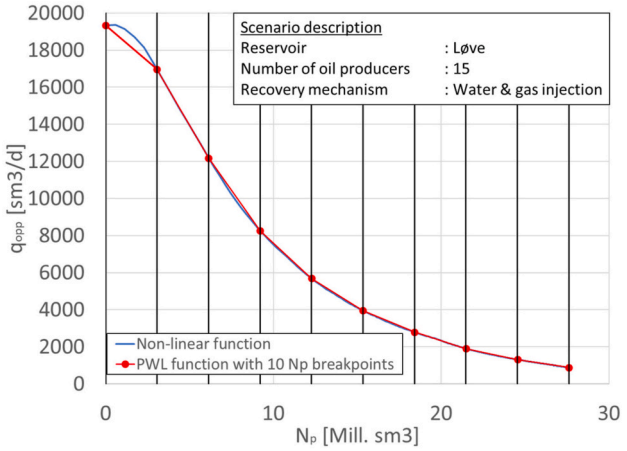

Fig. 4. An example of a PWL function constructed using ten N_p breakpoints to approximate a non-linear function.

$$E_{r,r}^{t,c} = \frac{\left| q_{o,r}^{t,c} - q_{o,r}^{t,ref} \right|}{q_{o,r}^{t,ref}} \tag{34}$$

where $E_{r,r}^{t,c}$: relative error for reservoir r at time t in case c, $q_{o,r}^{t,c}$ and $q_{o,r}^{t,ref}$: oil production rate of reservoir r at time t obtained in case c and in the reference case, respectively. The maximum E_r for all cases are summarized in Table 3. As shown in the table, the maximum E_r generally goes up when fewer N_p breakpoints are used. To maintain the accuracy of the optimization results, we define an upper limit for the maximum E_r, i.e., 10%. To meet this criteria, at least ten N_p breakpoints are needed. This "optimum" number of breakpoints has been adopted when reformulating and solving the optimization problems in Section 6.

The relationship between the number of N_p breakpoints and the optimization runtime is presented in Fig. 5. As shown in the figure, the runtime exponentially increases when the PWL approximation uses more N_p breakpoints. By reducing the number of N_p breakpoints from 30 to 10, we manage to make the optimization process 150 times faster.

8.2. Selecting the breakpoints for constructing the PWL functions

The use of a uniform spacing between the breakpoints can still lead to a poor fitting of the original non-linear function. An example of this is shown in Fig. 4 ($\forall N_p \in [0, 2]$ mill. sm^3). In the literature, there are some automated methods available for selecting breakpoints, such as ones presented by Hamann and Chen (1994); Hoffmann (2014). However, in this work, the N_p breakpoints are manually selected based on visual observation. The N_p breakpoints are chosen in such a way the difference between the non-linear function and its PWL approximation is minimal. Fig. 6 illustrates the PWL functions that are constructed using the manually selected breakpoints. The green circle in the figure indicates an improvement of the PWL function in representing the non-linear function. For a given number of breakpoints, a lower value of maximum E_r is anticipated when the manually-selected breakpoints are used instead of the uniformly-spaced breakpoints.

8.3. Evaluating approaches to compute the production and injection rates of gas and water

The optimization problems presented in this paper include the production and injection rates of gas and water as variables. The way these rates are estimated influences the total number of variables involved, and consequently the optimization runtime. For this reason, another investigation is carried out to identify the most efficient approach for computing these rates. In this investigation, we compare two methods for calculating the gas production rate.

The first method for calculating the gas production rate is inspired by the work of González et al. (2019). In this method, we first estimate the producing gas-oil ratio (GOR) of reservoir r at time t, $R_{p,r}^t$. This producing GOR is non-linearly dependent on (i) the reservoir, (ii) the recovery mechanism of the reservoir and (iii) the cumulative oil produced from the reservoir.

$$R_{p,r}^t = R_p\left(r, M_r, N_{p,r}^t\right) \tag{35}$$

The gas production rate of reservoir r at time t, $q_{g,r}^t$, is then obtained by multiplying the producing GOR with the corresponding oil production rate, $q_{o,r}^t$. This multiplication of variables makes the optimization model becomes an MINLP problem. To transform the optimization model into an MILP problem, another PWL function is established to approximate the non-linear function:

$$q_{g,r}^t = q_g\left(R_{p,r}^t, q_{o,r}^t\right) \tag{36}$$

In the second approach, we first estimate the cumulative gas produced from reservoir r at time t, $G_{p,r}^t$, and at time $t-1$, $G_{p,r}^{t-1}$. The cumulative gas production itself is a non-linear function of (i) the reservoir, (ii) the recovery mechanism of the reservoir and (iii) the cumulative oil produced from the reservoir.

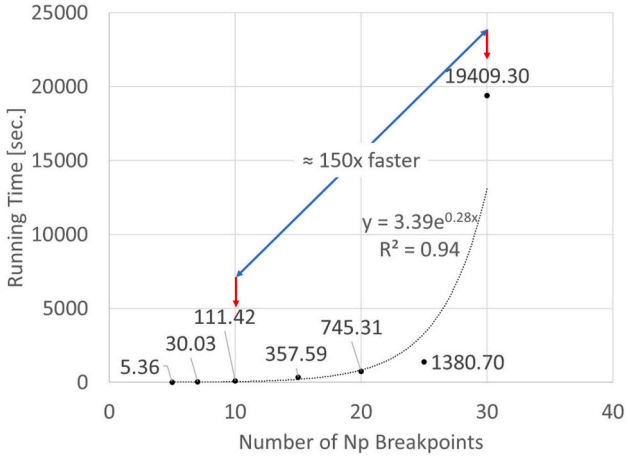

Fig. 5. Relationship between the number of N_p breakpoints and the optimization runtime.

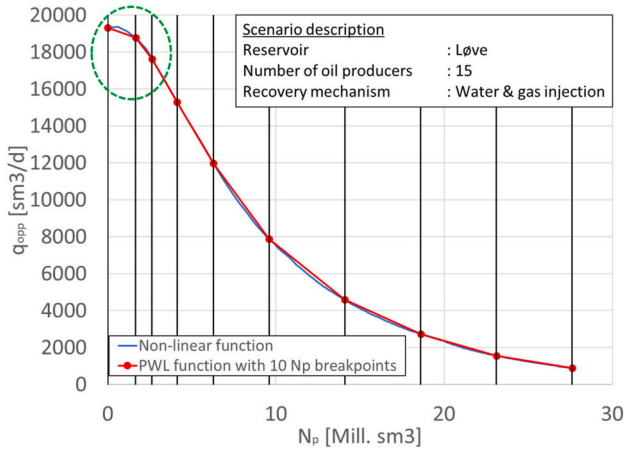

Fig. 6. An example of a PWL function constructed using ten manually-selected N_p breakpoints.

$$G^t_{p,r} = G_p\left(r, M_r, N^t_{p,r}\right) \tag{37}$$

The advantage of this approach is that the same SOS2 variables that are already in use for estimating $q^t_{opp,r}$ (Eq. (5)) can be utilized for estimating $G^t_{p,r}$. Thus, this approach introduces significantly fewer additional variables than the first approach.

The rate of gas production from reservoir r at time t, $q^t_{g,r}$, is then computed with a linear function that is dependent on the cumulative gas production of reservoir r at time $t-1$ and time t:

$$q^t_{g,r} = q_g\left(G^{t-1}_{p,r}, G^t_{p,r}\right) \tag{38}$$

The gas production profiles obtained from both methods are almost identical (see Fig. 7). There is, however, a minor discrepancy between the profiles. The reason might be an inaccurate approximation of the non-linear function $R^t_{p,r} = R_p(r, M_r, N^t_{p,r})$. Fig. 8 compares the runtime of optimization models implementing the two methods. The optimization process is considerably slower when the first method is used. It is because the implementation of the first method involves a lot of auxiliary variables for constructing the PWL function. Since the second method is computationally more efficient, the method is adopted in our optimization models. Furthermore, the idea of the second method is applied to estimate the water production rate, $q^t_{w,r}$, gas injection rate, $q^t_{gi,r}$, and water injection rate, $q^t_{wi,r}$.

8.4. Evaluating numerical integration techniques to compute the cumulative fluid production or injection

Authors investigate the use of two numerical integration techniques in the optimization model, i.e., the backward rectangular rule and the trapezoidal rule. For example, the cumulative gas production is estimated as the following if the backward rectangular rule is adopted:

$$G^t_{p,r} = G^{t-1}_{p,r} + \Delta t \cdot q^t_{g,r}, \quad \forall r \in R, \quad \forall t \in \{2, \ldots, n_t\} \tag{39}$$

When the trapezoidal rule is applied, the cumulative gas production is calculated as follows:

$$G^t_{p,r} = G^{t-1}_{p,r} + \Delta t \cdot \frac{q^{t-1}_{g,r} + q^t_{g,r}}{2}, \quad \forall r \in R, \quad \forall t \in \{2, \ldots, n_t\} \tag{40}$$

Fig. 9 compares the gas production profiles that are obtained from a case employing the backward rectangular rule and a case using the trapezoidal rule. As shown in this figure, the gas production rate oscillates severely in the case that employs the trapezoidal rule. A further investigation determines that the oscillations occur because we have an under-determined system, i.e., fewer equations than unknowns.

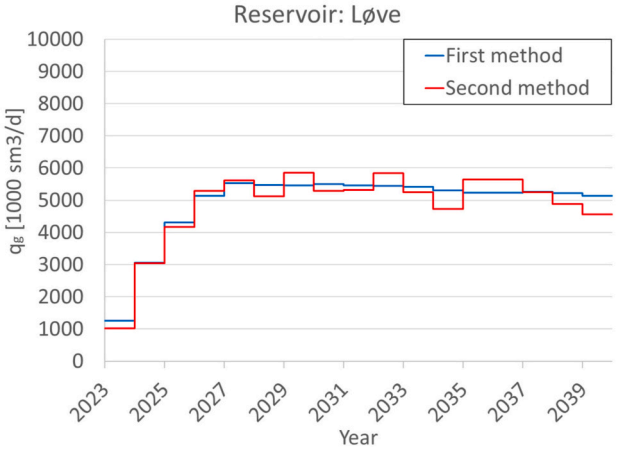

Fig. 7. Comparison of the gas production profile obtained from the two methods.

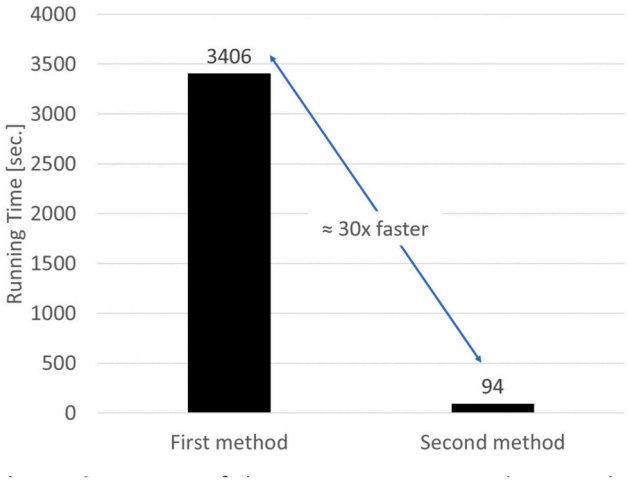

Fig. 8. Comparison of the optimization runtime between the cases applying the first method and the second method.

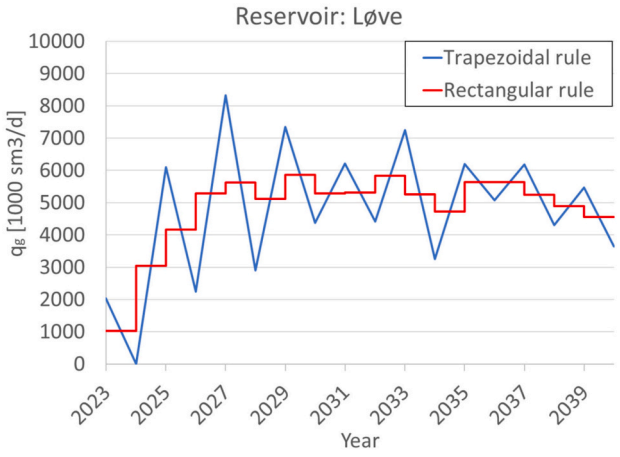

Fig. 9. Comparison of the gas production profile between the cases applying the rectangular rule and the trapezoidal rule.

Referring to Eq. (40), note that we use $n_t - 1$ equations ($t \in \{2,\ldots,n_t\}$) to determine the gas production rate at n_t points in time.

The oscillation issue does not emerge when the backward rectangular rule is applied. It is because $n_t - 1$ equations are used to determine the gas production rate at $n_t - 1$ points in time (see Eq. (39)). This numerical integration technique is therefore adopted in our optimization models for computing the cumulative fluid production or injection.

8.5. Optimizing the parallel computing

Parallel computing often helps to speed up the optimization process. Generally, the more the CPU cores involved, the faster the optimization process is. A study is performed to demonstrate how the number of CPU cores influences the optimization process. Four cases with different numbers of CPU cores are generated and run (see Table 4). The optimization process is terminated once the runtime reaches a specified time limit, i.e., 12 h. The objective value, optimality gap and runtime for each case are summarized in Table 4. By comparing these parameters, it is decided to use four CPU cores for solving the optimization problems.

8.6. Choosing the solver type

There are many solvers available to solve an MILP problem. A study was carried out to evaluate the performance of two extensively used

Table 4
Comparison of cases evaluated for optimizing the parallel computing.

CASE nr.	Objective function	Solver	Number of CPU cores	Objective value	Optimality gap	Runtime (h.)
10	max plateau duration	CPLEX	16	190947	5.91%	12
11	max plateau duration	CPLEX	8	190421	3.24%	12
12	max plateau duration	CPLEX	4	190421	1.55%	12
13	max plateau duration	CPLEX	2	190421	2.42%	12

solvers, namely: CPLEX and Gurobi. In this study, four cases are considered (see Table 5). The differences between the cases are only the objective function and the solver employed. CASE-14 and -15 are basically CASE-1 solved using CPLEX and Gurobi solver, respectively. Likewise, CASE-16 and -17 are CASE-2 solved using CPLEX and Gurobi solver, respectively. The solvers use almost all its default settings when solving the optimization problems. Like the previous study, the optimization process is also stopped after running for 12 h. The objective value, optimality gap and runtime for each case are summarized in Table 5. By comparing these parameters, it is concluded that Gurobi has a slightly better performance for solving the optimization problem to maximize plateau duration, whereas CPLEX performs better for solving the optimization problem to maximize NPV.

9. Uncertainties quantification

During field development planning, most of the inputs used for analysis are highly uncertain. In our case, the uncertainty of the optimization results originates from the imperfect information used for the optimization inputs. This section is focused on discussing how the uncertainties affect the optimization results, particularly for the optimization problem to maximize NPV.

9.1. Uncertain parameters

The uncertainty analysis presented in this paper considers three uncertain parameters, i.e., original oil-in-place (OOIP), development costs and oil price. The details of each uncertain parameter are provided as follows.

Variation of OOIP is expressed with the following equation:

$$N_r = U_N \cdot N_r^{base} \tag{41}$$

where N_r: OOIP of reservoir r, N_r^{base}: base value for OOIP of reservoir r, U_N: uncertainty factor for OOIP. The base value for OOIP of reservoir r is the one given in Appendix A, particularly in Table A.1. Distribution of the value of U_N is assumed to follow a normal distribution. The mean and standard deviation of the normal distribution are 1 and 0.2, respectively. Variation of OOIP does change the production potential curve and eventually affects the optimization results. Fig. 10 illustrates how the production potential curve changes as the OOIP varies. The production potential curve for each OOIP is obtained by running a simulation of the integrated production system model with the corresponding OOIP input. Referring to this figure, it is found that the production potential curve is stretched or squeezed in the horizontal direction proportionally to the change of OOIP. This means that if a reservoir has x% higher OOIP, the oil production potential (q_{opp}) will drop to a certain value after x% more oil has been produced. For example, in a reservoir with an OOIP of 75 million sm^3, the oil production potential drops to 5000 sm^3/d after the reservoir has produced 13.35 million sm^3 oil (see the green line in Fig. 10). Nevertheless, for a 40% larger reservoir (OOIP of 105 million sm^3), the oil production potential drops to 5000 sm^3/d after 18.7 million sm^3 (40% more) oil has been produced (see the red line in Fig. 10). This property is obtained from the fact that a larger reservoir has a slower production decline.

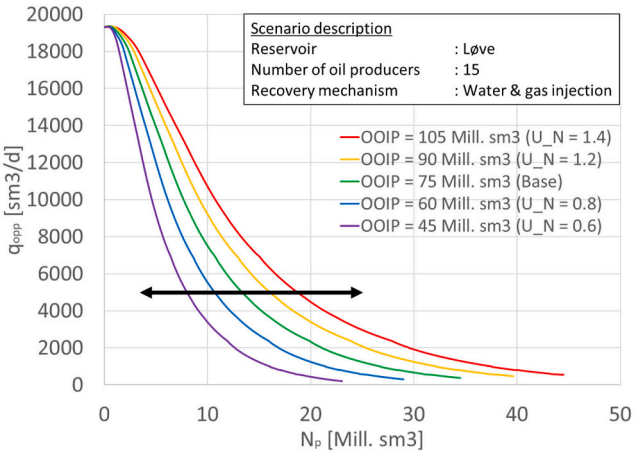

Fig. 10. Change of production potential curve with respect to OOIP.

The variation of OOIP has different implications and consequences on each optimization model. For the optimization model that maximizes plateau duration, a higher OOIP will result in a longer plateau period. For the optimization model that maximizes NPV, a higher OOIP allows the reservoir to be produced at higher plateau rates or at the same plateau rate for a longer time, thus increasing revenue. However, a higher OOIP also requires drilling more wells and having larger production capacities for the processing facility. Therefore, the OOIP greatly affects the optimal strategy to develop the field, where higher OOIPs usually lead to more aggressive field designs with bigger facilities, more wells, and higher production.

Variation of development costs is expressed with the following equation:

$$C_e = U_C \cdot C_e^{base} \tag{42}$$

where C_e: cost associated to cost element e, C_e^{base}: base value for cost associated to cost element e, U_C: uncertainty factor for development

Table 5
Comparison of cases evaluated for choosing the solver type.

CASE nr.	Objective function	Solver	Number of CPU cores	Objective value	Optimality gap	Runtime (h.)
14	max plateau duration	CPLEX	4	190421	1.55%	12
15	max plateau duration	Gurobi	4	190421	1.53%	12
16	max NPV	CPLEX	4	32068	16.88%	12
17	max NPV	Gurobi	4	32068	20.03%	12

costs. Again, the cost elements consist of EXPEX, DRILLEX, ABEX, CAPEX-SUB, CAPEX-TOP and OPEX. The base value for cost associated to cost element e is the one obtained from the cost proxy model (Appendix C). Distribution of the value of U_C is modeled with a normal distribution. The mean and standard deviation of the normal distribution are 1 and 0.2, respectively. This distribution type is common to use at the early stage of field development (Alexander Hall and Delille, 2011).

Variation of oil price is expressed with the following equation:

$$P_o = U_{P_o} \cdot P_o^{base} \tag{43}$$

where P_o: oil price, P_o^{base}: base value for oil price, U_{P_o}: uncertainty factor for oil price. The base value for oil price is 60 USD/bbl, and it is constant throughout the production period. Distribution of the value of U_{P_o} is modeled with a uniform distribution. The minimum and maximum of the uniform distribution are 0.4 and 1.6, respectively. This distribution type is chosen to represent a higher degree of uncertainty possessed by the oil price.

9.2. Uncertainty analysis

In this paper, uncertainty analyses are carried out using two approaches. The first uncertainty analysis uses the Latin hypercube sampling (LHS) method. This sampling method is preferred over the random sampling method because it can recreate the input probability distribution through fewer iterations. In other words, for the same number of iterations, the use of LHS method will provide more accurate uncertainty analysis results than the use of random sampling method. In the uncertainty analysis using the LHS method, we generate 100 samples, i.e., 100 combinations of U_N, U_C and U_{P_o}. The optimization is run for each one of these combinations.

The other method employed is a probability tree. To create the probability tree, we need to discretize the continuous probability distributions of the uncertainty factors U_N, U_C and U_{P_o}. To do so, we first define that each uncertainty factor has three possible values, i.e., equal to the values of P90, P50 and P10. The probability associated with each possible value or branch is then determined using a technique presented by McNamee and Celona (2008). In addition, the uncertainties of OOIP, development costs and oil price are independent of each other. The resulting probability tree is shown in Fig. 11. Referring to this probability tree, there are 3^3 combinations of U_N, U_C and U_{P_o}. Again, the optimization is run for each one of these combinations.

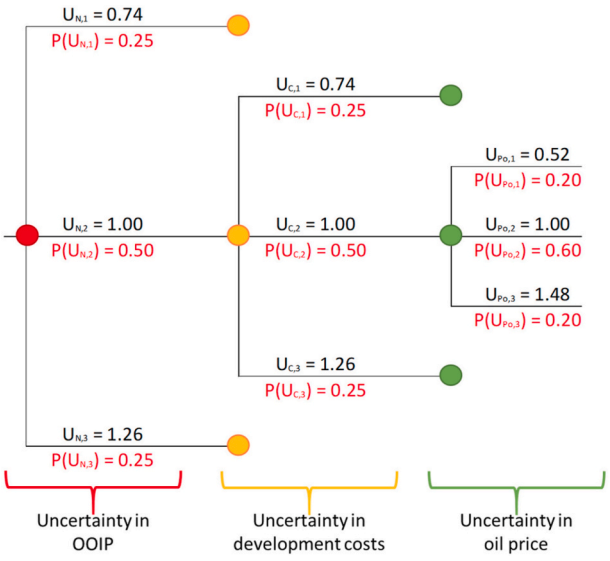

Fig. 11. Probability tree used in one of the uncertainty analyses.

9.3. Results of the uncertainty analysis

The results of the uncertainty analyses are presented using box plots. The box plot shows the P75, P50, P25 and average values of each variable (the number of wells or the field oil production rate for each time step). In addition to that, the box plot denotes a lower whisker, W_l, and an upper whisker, W_u. These whiskers cap the distribution and are typically defined as follows (Dümbgen and Riedwyl, 2007):

$$W_l = \max\{\min, (\mathrm{P75} - 1.5 \cdot \mathrm{IQR})\} \tag{44a}$$

$$W_u = \min\{\max, (\mathrm{P25} + 1.5 \cdot \mathrm{IQR})\} \tag{44b}$$

where IQR stands for interquartile range and is found as the difference between P25 and P75. For the uncertainty analysis using a probability tree, the expected value is computed and also presented in the box plot.

Distributions of the optimal drilling schedule and the optimal oil production profile obtained from both uncertainty analyses are shown in Figs. 12 and 13, respectively. In these figures, it can be observed that both uncertainty analyses produce almost similar results. The only notable difference is that the uncertainty analysis using a probability tree produces slightly narrower ranges of the lower and upper whiskers. This difference most likely originates from the discretization of the continuous probability distributions, where it misses the upper and lower extremes of the distributions. Considering the resemblance of results from both uncertainty analyses, the uncertainty analysis using a probability tree is preferred because it evaluates fewer cases, and thus requires a shorter time to complete. Note that this preference is valid only for the scope of uncertainty analysis performed in this study, i.e., involving only three uncertain parameters.

10. Conclusions

- A decision support methodology suitable for the early stage of the field planning process is presented. The methodology is applied on a synthetic field that has multiple non-communicating reservoir units producing independently to a common processing facility. The main part of the methodology is a mathematical optimization that uses (i) proxy models to represent the performance of the production system and to estimate the development costs and (ii) PWL approximations to represent some non-linear functions. In this study, the optimization models are aimed to maximize plateau duration or NPV by seeking the best configuration of production schedule, drilling schedule and recovery mechanism, while honoring several constraints.
- The optimization results denote that the objective value can be improved by considering more decision variables in the optimization problems. For example, including the drilling schedule and recovery mechanism as decision variables gives us 85% higher optimal NPV than optimizing the production schedule alone.
- Measures to speed up the optimization process and to ensure the accuracy of the optimization results are discussed. These measures have been implemented for formulating and solving the optimization problems.
- Uncertainty of the optimization results has been quantified through uncertainty analyses. These analyses consider three uncertain parameters, i.e., OOIP, development costs, and oil price. Two approaches have been evaluated for conducting the uncertainty analysis, i.e., using the LHS method and using a probability tree. The uncertainty analysis using a probability tree is recommended because it requires less time to complete while produces almost similar results as the LHS method.

Credit author statement

I Gusti Agung Gede Angga: Methodology; Software; Formal analysis;

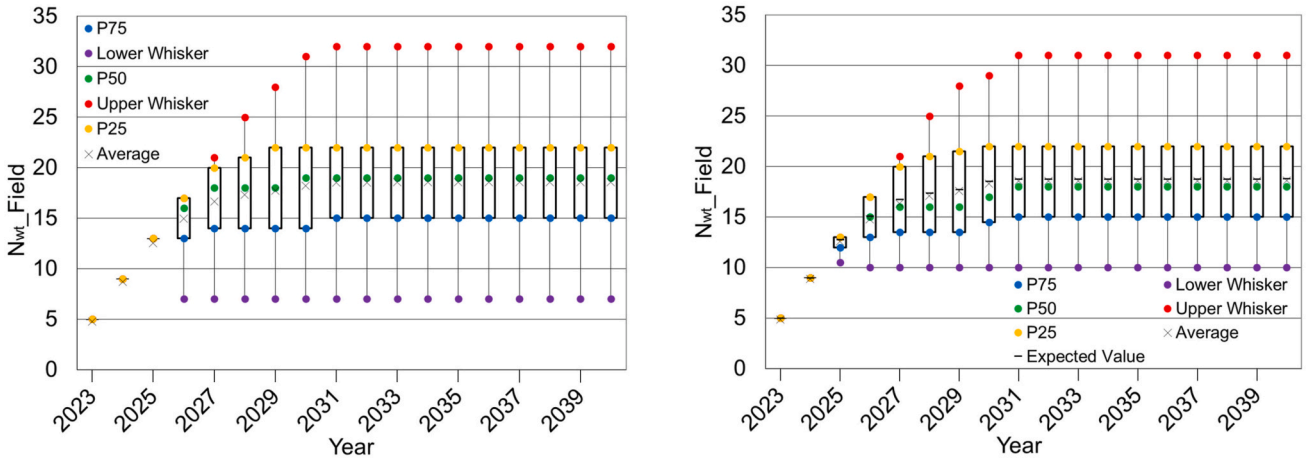

(a) Using the LHS method (b) Using a probability tree

Fig. 12. Distributions of the optimal drilling schedule obtained from the two uncertainty analyses.

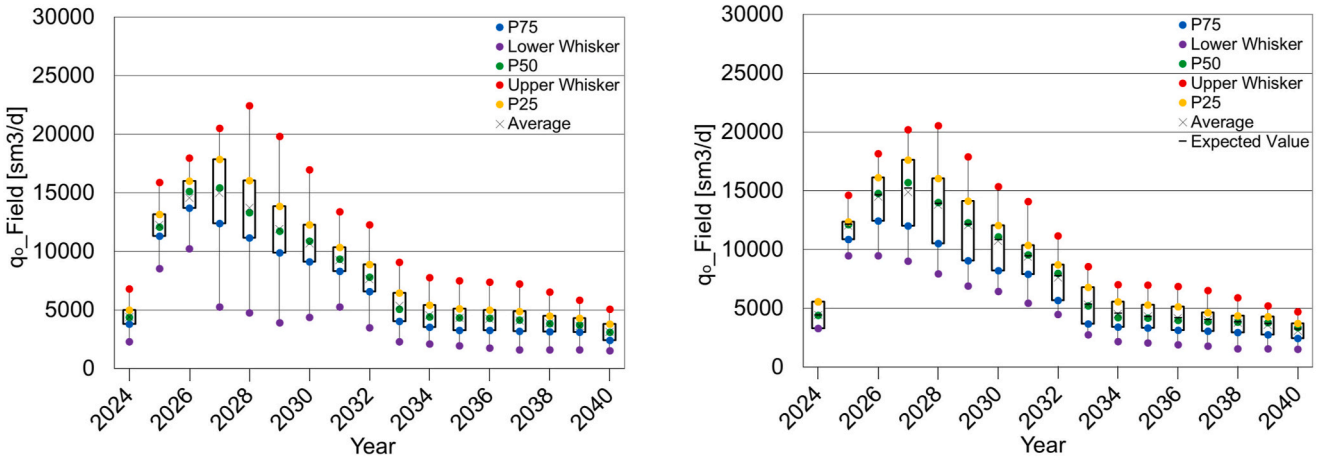

(a) Using the LHS method (b) Using a probability tree

Fig. 13. Distributions of the optimal oil production profile obtained from the two uncertainty analyses.

Investigation; Data curation; Visualization; Writing – original draft; Writing – review & editing. Milan Stanko: Conceptualization; Resources; Formal analysis; Investigation; Data curation; Writing – review & editing; Supervision; Project administration.

Declaration of competing interest

The authors declare that they have no known competing financial interests or personal relationships that could have appeared to influence the work reported in this paper.

Acknowledgments

The authors acknowledge the support from AkerSolutions, especially Thomas Førde, in providing a synthetic field case used for this work and input data for developing a proxy model for cost estimation. The authors also acknowledge the support from the Department of Geoscience and Petroleum of the Norwegian University of Science and Engineering (NTNU) in conducting this research.

Appendix A. Detailed Information about the Safari Field

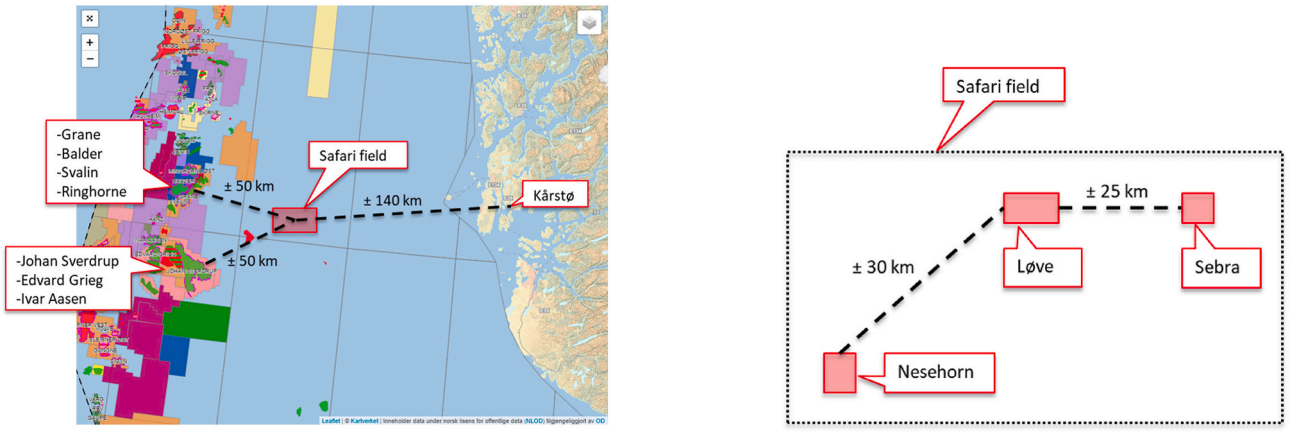

(a) Safari field (b) Reservoir units in Safari field

Fig. A.1. Location of Safari field and its reservoir units. The base figure is taken from NPD (2020).

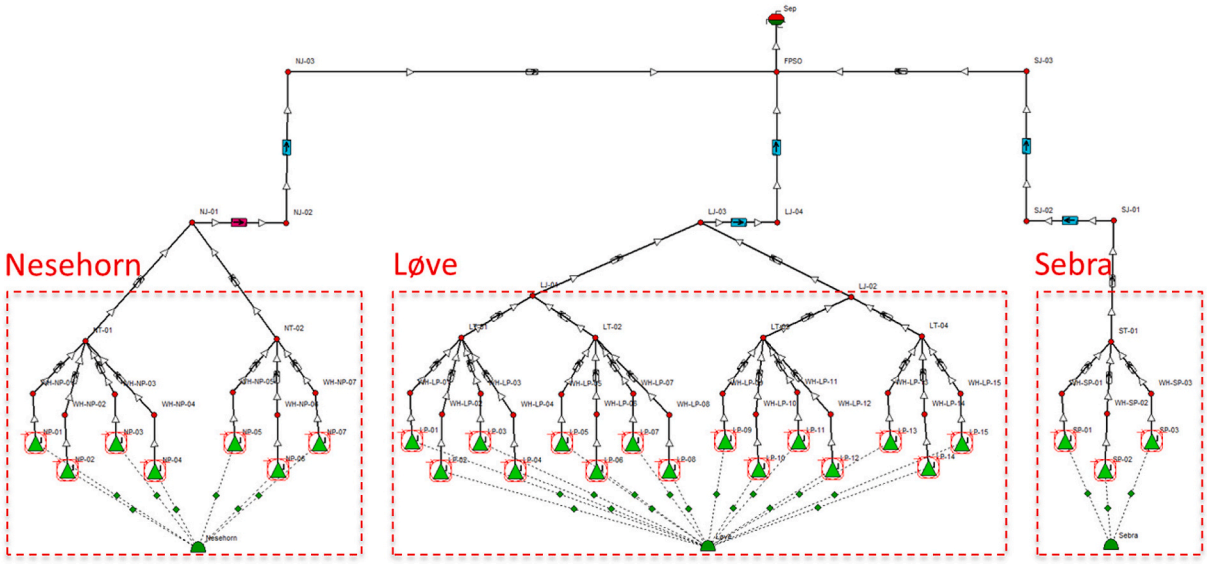

Fig. A.2. Layout of Safari field production system for the development using an FPSO

Table A.1
Initial reservoir condition & fluid properties

Parameter	Løve	Nesehorn	Sebra	Unit
Reservoir pressure	280	280	280	bara
Reservoir temperature	80	80	80	^{o}C
OOIP	75	55	13	Mill. sm^3
Aquifer volume	30	20	20	Mill. sm^3
Oil density	933.99	850	850	kg/m^3
Gas density	0.8	0.75	0.75	sp. gravity
Solution GOR	50	150	150	sm^3/sm^3
Saturation pressure	174.4	257.3	257.3	bara

Table A.2
Reservoir rock properties

Parameter	Løve	Nesehorn	Sebra	Unit
Permeability	250	250	450	mD
Porosity	0.18	0.18	0.18	
Reservoir thickness	50	50	50	m
Irreducible water saturation (S_{wirr})	0.25	0.25	0.25	

(*continued on next page*)

Table A.2 (*continued*)

Parameter	Løve	Nesehorn	Sebra	Unit
Residual oil saturation (S_{or})	0.25	0.25	0.25	
$k_{rw}@(1 - S_{or})$	0.8	0.8	0.8	
$k_{ro}@S_{wirr}$	0.8	0.8	0.8	
Corey exponent for water	1.5	1.5	1.5	
Corey exponent for oil	1.5	1.5	1.5	

Table A.3
Well properties

Parameter	Løve	Nesehorn	Sebra	Unit
Water depth	120	120	120	m
Well MD (TVD)	3500 (2500)	3500 (2500)	3500 (2500)	m
Wellbore radius	0.12	0.12	0.12	m
Well drainage radius	800	800	800	m
Skin factor	+5	+5	+5	
Tubing ID	0.124	0.124	0.124	m
Artificial lift	gas lift (GL)	GL	GL	
GL valve depth	3000	3000	3000	m
GL gas gravity	0.7	0.7	0.7	sp. gravity
GL maximum injection rate	400	400	400	1000 sm^3/d

Appendix B. Proxy Model of the Production System

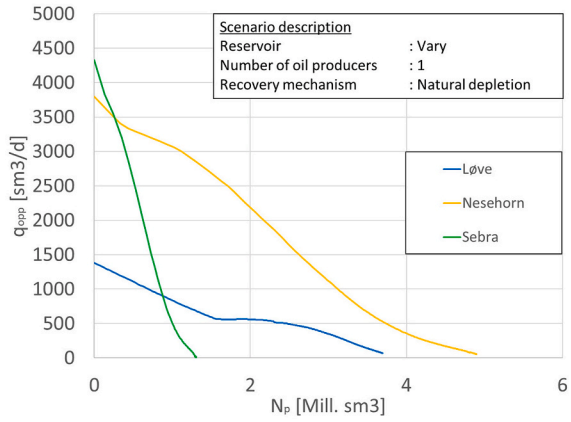

(a) Variation: reservoir unit

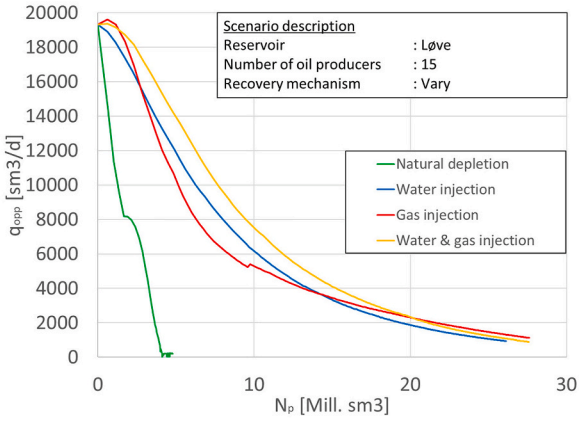

(b) Variation: recovery mechanism

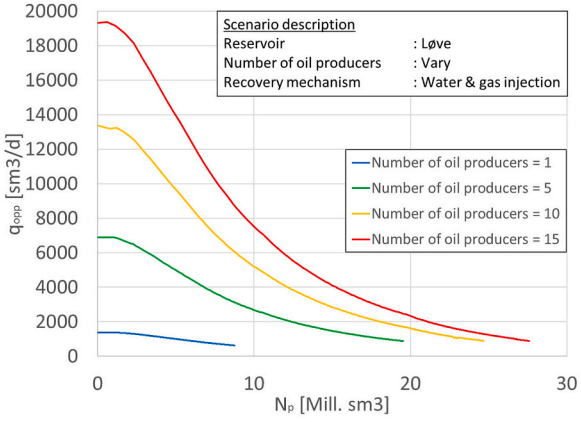

(c) Variation: number of oil producers

Fig. B.1. Examples of the production potential curve

Appendix C. Proxy Model for Cost Estimation

EXPEX: The future value of EXPEX, $F_{v,ex}$, is calculated as follows:

$$F_{v,ex} = \sum_{t\in\{-3,-2,\ldots,0\}} A_t \tag{C.1}$$

where A_t is a constant. The value of this constant is given in Table C.1. The distribution of EXPEX is summarized in Table C.2. The non-positive time index t (in Table C.2 to Table C.5 and Appendix F) correlates with the number of years before the field production starts.

DRILLEX: The future value of DRILLEX made at time t, $F^t_{v,dx}$, is calculated as follows:

$$F^t_{v,dx} = B\cdot\left(N^{t+1}_{wt,f} - N^t_{wt,f}\right) \tag{C.2}$$

where B indicates the drilling cost for a well, and the term $(N^{t+1}_{wt,f} - N^t_{wt,f})$ represents the number of wells drilled from time t to $t+1$. The value of coefficient B is given in Table C.1.

ABEX: The future value of ABEX, $F_{v,ax}$, is calculated as follows:

$$F_{v,ax} = \left(\sum_{t\in\{-3,-2,\ldots,0\}} C_t\right) + D_1\cdot N^{n_t}_{op,f} + D_2\cdot\left(N^{n_t}_{gi,f} + N^{n_t}_{wi,f}\right) \tag{C.3}$$

where $N^{n_t}_{op,f}$, $N^{n_t}_{gi,f}$ and $N^{n_t}_{wi,f}$ are the numbers of oil producers, gas injectors and water injectors, respectively, at the end of the field lifetime. C_t is a constant, while D_1 and D_2 are coefficients. The values of these constant and coefficients are given in Table C.1. The distribution of ABEX is summarized in Table C.3. Note that the amounts of ABEX are in reality executed after the field stops producing. However, the amounts presented (in Table C.3) are the discounted amounts as if they are executed before the production period.

CAPEX-SUB: The future value of CAPEX-SUB, $F_{v,sx}$, is calculated as follows:

$$F_{v,sx} = E_1\cdot N_{st,f} + E_2\cdot N_{xt,f} \tag{C.4}$$

where $N_{st,f}$ and $N_{xt,f}$ are the numbers of subsea templates and subsea xmas trees in the field, respectively. E_1 and E_2 are coefficients, and their values are given in Table C.1. The distribution of CAPEX-SUB is summarized in Table C.4.

CAPEX-TOP: The future value of CAPEX-TOP, $F_{v,tx}$, is calculated as follows:

$$F_{v,tx} = G_1\cdot q_o^{capacity} + G_2\cdot q_g^{capacity} + G_3\cdot q_w^{capacity} \tag{C.5}$$

where $q_o^{capacity}$, $q_g^{capacity}$ and $q_w^{capacity}$ are the capacities of the processing facility to handle oil, gas and water production, respectively. G_1, G_2 and G_3 are coefficients, and their values are given in Table C.1. The distribution of CAPEX-TOP is summarized in Table C.5.

OPEX: The future value of OPEX spent at time t, $F^t_{v,ox}$, is calculated as follows:

$$F^t_{v,ox} = H_1 + H_2\cdot N^{t-1}_{op,f} + H_3\cdot q^t_{o,f} + H_4\cdot q^t_{g,f} + H_5\cdot q^t_{w,f} \tag{C.6}$$

where $N^{t-1}_{op,f}$ represents the number of oil producers available for maintenance, while $q^t_{o,f}$, $q^t_{g,f}$ and $q^t_{w,f}$ represent the average production rates of oil, gas and water, respectively, from time $t-1$ to t. H_1 is a constant, while H_2, H_3, H_4 and H_5 are coefficients. The values of these constant and coefficients are given in Table C.1.

Table C.1
Values of constants and coefficients used in the cost proxy model

Constant/Coefficient	Value	Unit
A_{-3}	665	Mill. NOK
A_{-2}	240	Mill. NOK
A_{-1}	380	Mill. NOK
A_0	366	Mill. NOK
B	480	Mill. NOK/well
C_{-3}	192	Mill. NOK
C_{-2}	449	Mill. NOK
C_{-1}	449	Mill. NOK
C_0	192	Mill. NOK
D_1	12	Mill. NOK/oil producer
D_2	5	Mill. NOK/injector
E_1	484	Mill. NOK/template
E_2	50	Mill. NOK/xmas tree
G_1	0.10914	Mill. NOK/(sm^3/d)
G_2	0.23848	Mill. NOK/(1000 sm^3/d)
G_3	0.22074	Mill. NOK/(sm^3/d)
H_1	400	Mill. NOK

(continued on next page)

Table C.1 (*continued*)

Constant/Coefficient	Value	Unit
H_2	4	Mill. NOK/oil producer
H_3	0.007388	Mill. NOK/(sm^3/d)
H_4	0.018289	Mill. NOK/(1000 sm^3/d)
H_5	0.022829	Mill. NOK/(sm^3/d)

Table C.2
Distribution of EXPEX

t	Date of Expenditure	Expenditure
−3	1st Jan 2019	A_{-3}
−2	1st Jan 2020	A_{-2}
−1	1st Jan 2021	A_{-1}
0	1st Jan 2022	A_0

Table C.3
Distribution of ABEX

t	Date of Expenditure	Expenditure
−3	1st Jan 2019	$C_{-3} + D_1 \cdot N_{op,f}^{n_t} + D_2 \cdot (N_{gi,f}^{n_t} + N_{wi,f}^{n_t})$
−2	1st Jan 2020	C_{-2}
−1	1st Jan 2021	C_{-1}
0	1st Jan 2022	C_0

Table C.4
Distribution of CAPEX-SUB

t	Date of Expenditure	Expenditure
−3	1st Jan 2019	$F_{v,sx}/4$
−2	1st Jan 2020	$F_{v,sx}/4$
−1	1st Jan 2021	$F_{v,sx}/4$
0	1st Jan 2022	$F_{v,sx}/4$

Table C.5
Distribution of CAPEX-TOP

t	Date of Expenditure	Expenditure
−3	1st Jan 2019	$F_{v,tx}/4$
−2	1st Jan 2020	$F_{v,tx}/4$
−1	1st Jan 2021	$F_{v,tx}/4$
0	1st Jan 2022	$F_{v,tx}/4$

Appendix D. Description of Optimization Parameters, Sets and Variables

Table D.1
Optimization parameters

Parameter	Description
n_r	Number of reservoir units in the field
n_t	Number of time steps
t_{up}	Number of operational days per year
$q_{o,f}^{plateau}$	Desired plateau rate for the field oil production (unit: sm^3/d)
$q_{gi}^{capability}$	Maximum gas injection rate of a gas injector (unit: 1000 sm^3/d)
$q_{wi}^{capability}$	Maximum water injection rate of a water injector (unit: sm^3/d)
$N_{op}^{pre-drilled}$	Maximum number of pre-drilled oil producers

(*continued on next page*)

Table D.1 (*continued*)

Parameter	Description
$N_{it}^{pre-drilled}$	Maximum number of pre-drilled injectors
$N_{wt}^{max-drilled}$	Maximum number of wells drilled each year
$N_{gi,r}^{max}$	Maximum number of gas injectors drilled in reservoir r
$N_{wi,r}^{max}$	Maximum number of water injectors drilled in reservoir r
d	Yearly discount rate
P_o	Oil price (unit: USD/bbl)
X_r	Exchange rate (unit: NOK/USD)
X_v	Volume conversion constant (unit: bbl/m^3)

Table D.2
Sets of reservoirs and time steps

Set	Description
R	Set of all reservoir units
T	Set of all time steps

Table D.3
Reservoir variables

Variable	Description
M_r	Recovery mechanism of reservoir r
$q_{opp,r}^t$	Oil production potential of reservoir r at time t (unit: sm^3/d)
$q_{o,r}^t$	Oil production rate of reservoir r at time t (unit: sm^3/d)
$q_{g,r}^t$	Gas production rate of reservoir r at time t (unit: 1000 sm^3/d)
$q_{w,r}^t$	Water production rate of reservoir r at time t (unit: sm^3/d)
$q_{gi,r}^t$	Gas injection rate of reservoir r at time t (unit: 1000 sm^3/d)
$q_{wi,r}^t$	Water injection rate of reservoir r at time t (unit: sm^3/d)
$N_{p,r}^t$	Cumulative oil production of reservoir r at time t (unit: Mill. sm^3)
$G_{p,r}^t$	Cumulative gas production of reservoir r at time t (unit: Mill. sm^3)
$W_{p,r}^t$	Cumulative water production of reservoir r at time t (unit: Mill. sm^3)
$G_{i,r}^t$	Cumulative gas injection of reservoir r at time t (unit: Mill. sm^3)
$W_{i,r}^t$	Cumulative water injection of reservoir r at time t (unit: Mill. sm^3)
$N_{op,r}^t$	Number of oil producers in reservoir r at time t
$N_{gi,r}^t$	Number of gas injectors in reservoir r at time t
$N_{wi,r}^t$	Number of water injectors in reservoir r at time t
$N_{wt,r}^t$	Number of wells in reservoir r at time t
$N_{st,r}$	Number of subsea templates in reservoir r
$z_{gi,r}$	Binary variable which the value depends on the recovery mechanism of reservoir r
$z_{wi,r}$	Binary variable which the value depends on the recovery mechanism of reservoir r

Table D.4
Field variables

Variable	Description
$q_{opp,f}^t$	Field oil production potential at time t (unit: sm^3/d)
$q_{o,f}^t$	Field oil production rate at time t (unit: sm^3/d)
$q_{g,f}^t$	

(*continued on next page*)

Table D.4 (*continued*)

Variable	Description
	Field gas production rate at time t (unit: 1000 sm^3/d)
$q^t_{w,f}$	Field water production rate at time t (unit: sm^3/d)
$q^t_{gi,f}$	Field gas injection rate at time t (unit: 1000 sm^3/d)
$q^t_{wi,f}$	Field water injection rate at time t (unit: sm^3/d)
$N^t_{p,f}$	Cumulative oil production of the field at time t (unit: Mill. sm^3)
$G^t_{p,f}$	Cumulative gas production of the field at time t (unit: Mill. sm^3)
$W^t_{p,f}$	Cumulative water production of the field at time t (unit: Mill. sm^3)
$G^t_{i,f}$	Cumulative gas injection of the field at time t (unit: Mill. sm^3)
$W^t_{i,f}$	Cumulative water injection of the field at time t (unit: Mill. sm^3)
$N^t_{op,f}$	Number of oil producers in the field at time t
$N^t_{gi,f}$	Number of gas injectors in the field at time t
$N^t_{wi,f}$	Number of water injectors in the field at time t
$N^t_{wt,f}$	Number of wells in the field at time t
$N_{st,f}$	Number of subsea templates in the field
$N_{xt,f}$	Number of subsea xmas trees in the field

Table D.5
Sets of breakpoints used in the MILP formulations

Set	Description
V_{N_p}	Set of cumulative oil production (N_p) breakpoints
$V_{N_{op,r}}$	Set of number of oil producers (N_{op}) breakpoints for reservoir r
V_{M_r}	Set of recovery mechanism (M) breakpoints for reservoir r

Table D.6
Breakpoints used in the MILP formulations

Parameter	Description
$\widehat{N^{j,k,l}_{p,r}}$	Cumulative oil production of reservoir r at breakpoint (j,k,l)
$\widehat{N^{j,k,l}_{op,r}}$	Number of oil producers in reservoir r at breakpoint (j,k,l)
$\widehat{M^{j,k,l}_{r}}$	Recovery mechanism of reservoir r at breakpoint (j,k,l)
$\widehat{q^{j,k,l}_{opp,r}}$	Oil production potential of reservoir r at breakpoint (j,k,l)
$\widehat{G^{j,k,l}_{p,r}}$	Cumulative gas production of reservoir r at breakpoint (j,k,l)
$\widehat{W^{j,k,l}_{p,r}}$	Cumulative water production of reservoir r at breakpoint (j,k,l)
$\widehat{G^{j,k,l}_{i,r}}$	Cumulative gas injection of reservoir r at breakpoint (j,k,l)
$\widehat{W^{j,k,l}_{i,r}}$	Cumulative water injection of reservoir r at breakpoint (j,k,l)
$\overline{z^{m,n}_{gi}}$	Value of binary variable z_{gi} at breakpoint (m,n)
$\overline{z^{m,n}_{wi}}$	Value of binary variable z_{wi} at breakpoint (m,n)
$\overline{M^{m,n}}$	Recovery mechanism at breakpoint (m,n)

Table D.7
Auxiliary variables used in the MILP formulations

Variable	Description
$\lambda_{r,t}^{j,k,l}$	Weighting variable for breakpoint (j,k,l), for reservoir r at time t
$\alpha_{r,t}^{j}$	SOS2 variable for breakpoint j, for reservoir r at time t
$\beta_{r,t}^{k}$	SOS2 variable for breakpoint k, for reservoir r at time t
$\gamma_{r,t}^{l}$	SOS1 variable for breakpoint l, for reservoir r at time t
$\omega_{r}^{m,n}$	Weighting variable for breakpoint (m,n), for reservoir r
ψ_{r}^{m}	SOS1 variable for breakpoint m, for reservoir r
τ_{r}^{n}	SOS1 variable for breakpoint n, for reservoir r

Table D.8
Economic variables

Variable	Description
$P_{v,ex}$	Present value of EXPEX (unit: Mill. NOK)
$P_{v,dx}^{pre-drilled}$	Present value of DRILLEX for pre-drilled wells (unit: Mill. NOK)
$P_{v,dx}^{t}$	Present value of DRILLEX made at time t (unit: Mill. NOK)
$P_{v,ax}$	Present value of ABEX (unit: Mill. NOK)
$P_{v,sx}$	Present value of CAPEX-SUB (unit: Mill. NOK)
$F_{v,tx}$	Future value of CAPEX-TOP (unit: Mill. NOK)
$P_{v,tx}$	Present value of CAPEX-TOP (unit: Mill. NOK)
$F_{v,ox}^{t}$	Future value of OPEX spent at time t (unit: Mill. NOK)
$P_{v,ox}^{t}$	Present value of OPEX spent at time t (unit: Mill. NOK)
$P_{v,re}^{t}$	Present value of revenue obtained at time t (unit: Mill. NOK)
$P_{v,pp}$	Present value of all expenditures made before the field enters the production period (unit: Mill. NOK)
D_{cf}^{t}	Discounted cash flow at time t (unit: Mill. NOK)
NPV	Net present value (unit: Mill. NOK)

Table D.9
Other variables

Variable	Description
$q_{o}^{capacity}$	Capacity of the processing facility to handle oil production (unit: sm^3/d)
$q_{g}^{capacity}$	Capacity of the processing facility to handle gas production (unit: 1000 sm^3/d)
$q_{w}^{capacity}$	Capacity of the processing facility to handle water production (unit: sm^3/d)

Appendix E. MILP Formulation of the Optimization Problem to Maximize Field Plateau Duration

Objective function:

$$\text{minimize} \quad \sum_{t\in\{2,\ldots,n_t\}} \left(q_{o,f}^{plateau} - q_{o,f}^{t}\right) \tag{E.1}$$

Operational constrains:

$$q_{o,f}^{t} \le q_{o,f}^{plateau}, \quad \forall t \in \{2,\ldots,n_t\} \tag{E.2}$$

$$q_{o,r}^{t} \le q_{opp,r}^{t}, \quad \forall r \in R \quad \text{and} \quad \forall t \in \{2,\ldots,n_t\} \tag{E.3}$$

$$q_{o,r}^{t} \le q_{opp,r}^{t-1}, \quad \forall r \in R \quad \text{and} \quad \forall t \in \{2,\ldots,n_t\} \tag{E.4}$$

$$q^t_{gi,r} \le N^{t-1}_{gi,r} \cdot q^{capability}_{gi}, \quad \forall r \in R \quad \text{and} \quad \forall t \in \{2, \ldots, n_t\} \tag{E.5}$$

$$q^t_{wi,r} \le N^{t-1}_{wi,r} \cdot q^{capability}_{wi}, \quad \forall r \in R \quad \text{and} \quad \forall t \in \{2, \ldots, n_t\} \tag{E.6}$$

Drilling constraints:

$$N^{t-1}_{op,r} \le N^t_{op,r}, \quad \forall r \in R \quad \text{and} \quad \forall t \in \{2, \ldots, n_t\} \tag{E.7}$$

$$N^{t-1}_{gi,r} \le N^t_{gi,r}, \quad \forall r \in R \quad \text{and} \quad \forall t \in \{2, \ldots, n_t\} \tag{E.8}$$

$$N^{t-1}_{wi,r} \le N^t_{wi,r}, \quad \forall r \in R \quad \text{and} \quad \forall t \in \{2, \ldots, n_t\} \tag{E.9}$$

$$N^t_{gi,r} \le z_{gi,r} \cdot N^{max}_{gi,r}, \quad \forall r \in R \quad \text{and} \quad \forall t \in T \tag{E.10}$$

$$N^t_{wi,r} \le z_{wi,r} \cdot N^{max}_{wi,r}, \quad \forall r \in R \quad \text{and} \quad \forall t \in T \tag{E.11}$$

$$N^1_{op,f} \le N^{pre-drilled}_{op} \tag{E.12}$$

$$N^1_{gi,f} + N^1_{wi,f} \le N^{pre-drilled}_{it} \tag{E.13}$$

$$N^t_{wt,f} - N^{t-1}_{wt,f} \le N^{max-drilled}_{wt}, \quad \forall t \in \{2, \ldots, n_t\} \tag{E.14}$$

Equality constraints:

$$N^1_{p,r} = 0, \quad \forall r \in R \tag{E.15}$$

$$N^t_{p,r} = N^{t-1}_{p,r} + \frac{t_{up} \cdot q^t_{o,r}}{10^6}, \quad \forall r \in R \quad \text{and} \quad \forall t \in \{2, \ldots, n_t\} \tag{E.16}$$

$$G^t_{p,r} = G^{t-1}_{p,r} + \frac{t_{up} \cdot q^t_{g,r}}{10^3}, \quad \forall r \in R \quad \text{and} \quad \forall t \in \{2, \ldots, n_t\} \tag{E.17}$$

$$W^t_{p,r} = W^{t-1}_{p,r} + \frac{t_{up} \cdot q^t_{w,r}}{10^6}, \quad \forall r \in R \quad \text{and} \quad \forall t \in \{2, \ldots, n_t\} \tag{E.18}$$

$$G^t_{i,r} = G^{t-1}_{i,r} + \frac{t_{up} \cdot q^t_{gi,r}}{10^3}, \quad \forall r \in R \quad \text{and} \quad \forall t \in \{2, \ldots, n_t\} \tag{E.19}$$

$$W^t_{i,r} = W^{t-1}_{i,r} + \frac{t_{up} \cdot q^t_{wi,r}}{10^6}, \quad \forall r \in R \quad \text{and} \quad \forall t \in \{2, \ldots, n_t\} \tag{E.20}$$

$$N^t_{wt,r} = N^t_{op,r} + N^t_{gi,r} + N^t_{wi,r}, \quad \forall r \in R \quad \text{and} \quad \forall t \in T \tag{E.21}$$

$$N^t_{op,f} = \sum_{r \in R} N^t_{op,r}, \quad \forall t \in T \tag{E.22}$$

$$N^t_{gi,f} = \sum_{r \in R} N^t_{gi,r}, \quad \forall t \in T \tag{E.23}$$

$$N^t_{wi,f} = \sum_{r \in R} N^t_{wi,r}, \quad \forall t \in T \tag{E.24}$$

$$N^t_{wt,f} = \sum_{r \in R} N^t_{wt,r}, \quad \forall t \in T \tag{E.25}$$

$$q^t_{opp,f} = \sum_{r \in R} q^t_{opp,r}, \quad \forall t \in T \tag{E.26}$$

$$q^t_{o,f} = \sum_{r \in R} q^t_{o,r}, \quad \forall t \in \{2, \ldots, n_t\} \tag{E.27}$$

$$q^t_{g,f} = \sum_{r \in R} q^t_{g,r}, \quad \forall t \in \{2, \ldots, n_t\} \tag{E.28}$$

$$q^t_{w,f} = \sum_{r \in R} q^t_{w,r}, \quad \forall t \in \{2, \ldots, n_t\} \tag{E.29}$$

$$q^t_{gi,f} = \sum_{r \in R} q^t_{gi,r}, \quad \forall t \in \{2, \ldots, n_t\} \tag{E.30}$$

$$q^t_{wi,f} = \sum_{r \in R} q^t_{wi,r}, \quad \forall t \in \{2, \ldots, n_t\} \tag{E.31}$$

$$N_{p,f}^{t} = \sum_{r \in R} N_{p,r}^{t}, \quad \forall t \in T \tag{E.32}$$

$$G_{p,f}^{t} = \sum_{r \in R} G_{p,r}^{t}, \quad \forall t \in T \tag{E.33}$$

$$W_{p,f}^{t} = \sum_{r \in R} W_{p,r}^{t}, \quad \forall t \in T \tag{E.34}$$

$$G_{i,f}^{t} = \sum_{r \in R} G_{i,r}^{t}, \quad \forall t \in T \tag{E.35}$$

$$W_{i,f}^{t} = \sum_{r \in R} W_{i,r}^{t}, \quad \forall t \in T \tag{E.36}$$

Constraints induced by PWL approximations:

$$N_{p,r}^{t} = \sum_{j \in V_{N_p}} \sum_{k \in V_{N_{op,r}}} \sum_{l \in V_{M_r}} \lambda_{r,t}^{j,k,l} \cdot \widehat{N_{p,r}^{j,k,l}}, \quad \forall r \in R, \forall t \in T \tag{E.37}$$

$$N_{op,r}^{t} = \sum_{j \in V_{N_p}} \sum_{k \in V_{N_{op,r}}} \sum_{l \in V_{M_r}} \lambda_{r,t}^{j,k,l} \cdot \widehat{N_{op,r}^{j,k,l}}, \quad \forall r \in R, \forall t \in T \tag{E.38}$$

$$M_{r} = \sum_{j \in V_{N_p}} \sum_{k \in V_{N_{op,r}}} \sum_{l \in V_{M_r}} \lambda_{r,t}^{j,k,l} \cdot \widehat{M_{r}^{j,k,l}}, \quad \forall r \in R, \forall t \in T \tag{E.39}$$

$$q_{opp,r}^{t} = \sum_{j \in V_{N_p}} \sum_{k \in V_{N_{op,r}}} \sum_{l \in V_{M_r}} \lambda_{r,t}^{j,k,l} \cdot \widehat{q_{opp,r}^{j,k,l}}, \quad \forall r \in R, \forall t \in T \tag{E.40}$$

$$1 = \sum_{j \in V_{N_p}} \sum_{k \in V_{N_{op,r}}} \sum_{l \in V_{M_r}} \lambda_{r,t}^{j,k,l}, \quad \forall r \in R, \forall t \in T \tag{E.41}$$

$$\alpha_{r,t}^{j} = \sum_{k \in V_{N_{op,r}}} \sum_{l \in V_{M_r}} \lambda_{r,t}^{j,k,l}, \quad \forall r \in R, \forall t \in T, \forall j \in V_{N_p} \tag{E.42}$$

$$\beta_{r,t}^{k} = \sum_{j \in V_{N_p}} \sum_{l \in V_{M_r}} \lambda_{r,t}^{j,k,l}, \quad \forall r \in R, \forall t \in T, \forall k \in V_{N_{op,r}} \tag{E.43}$$

$$\gamma_{r,t}^{l} = \sum_{j \in V_{N_p}} \sum_{k \in V_{N_{op,r}}} \lambda_{r,t}^{j,k,l}, \quad \forall r \in R, \forall t \in T, \forall l \in V_{M_r} \tag{E.44}$$

$$\left\{ \alpha_{r,t}^{j}, \quad j \in V_{N_p} \right\} \text{ is SOS2}, \quad \forall r \in R, \forall t \in T \tag{E.45}$$

$$\left\{ \beta_{r,t}^{k}, \quad k \in V_{N_{op,r}} \right\} \text{ is SOS2}, \quad \forall r \in R, \forall t \in T \tag{E.46}$$

$$\left\{ \gamma_{r,t}^{l}, \quad l \in V_{M_r} \right\} \text{ is SOS1}, \quad \forall r \in R, \forall t \in T \tag{E.47}$$

$$G_{p,r}^{t} = \sum_{j \in V_{N_p}} \sum_{k \in V_{N_{op,r}}} \sum_{l \in V_{M_r}} \lambda_{r,t}^{j,k,l} \cdot \widehat{G_{p,r}^{j,k,l}}, \quad \forall r \in R, \forall t \in T \tag{E.48}$$

$$W_{p,r}^{t} = \sum_{j \in V_{N_p}} \sum_{k \in V_{N_{op,r}}} \sum_{l \in V_{M_r}} \lambda_{r,t}^{j,k,l} \cdot \widehat{W_{p,r}^{j,k,l}}, \quad \forall r \in R, \forall t \in T \tag{E.49}$$

$$G_{i,r}^{t} = \sum_{j \in V_{N_p}} \sum_{k \in V_{N_{op,r}}} \sum_{l \in V_{M_r}} \lambda_{r,t}^{j,k,l} \cdot \widehat{G_{i,r}^{j,k,l}}, \quad \forall r \in R, \forall t \in T \tag{E.50}$$

$$W_{i,r}^{t} = \sum_{j \in V_{N_p}} \sum_{k \in V_{N_{op,r}}} \sum_{l \in V_{M_r}} \lambda_{r,t}^{j,k,l} \cdot \widehat{W_{i,r}^{j,k,l}}, \quad \forall r \in R, \forall t \in T \tag{E.51}$$

$$z_{gi,r} = \sum_{m \in \{1,2\}} \sum_{n \in \{1,2\}} \omega_{r}^{m,n} \cdot \overline{z_{gi}^{m,n}}, \quad \forall r \in R \tag{E.52}$$

$$z_{wi,r} = \sum_{m \in \{1,2\}} \sum_{n \in \{1,2\}} \omega_{r}^{m,n} \cdot \overline{z_{wi}^{m,n}}, \quad \forall r \in R \tag{E.53}$$

$$M_{r} = \sum_{m \in \{1,2\}} \sum_{n \in \{1,2\}} \omega_{r}^{m,n} \cdot \overline{M^{m,n}}, \quad \forall r \in R \tag{E.54}$$

$$1 = \sum_{m\in\{1,2\}} \sum_{n\in\{1,2\}} \omega_r^{m,n}, \quad \forall r \in R \tag{E.55}$$

$$\psi_r^m = \sum_{n\in\{1,2\}} \omega_r^{m,n}, \quad \forall r \in R, \quad \forall m \in \{1,2\} \tag{E.56}$$

$$\tau_r^n = \sum_{m\in\{1,2\}} \omega_r^{m,n}, \quad \forall r \in R, \quad \forall n \in \{1,2\} \tag{E.57}$$

$$\left\{\psi_r^1, \psi_r^2\right\} \text{ is SOS1}, \quad \forall r \in R \tag{E.58}$$

$$\left\{\tau_r^1, \tau_r^2\right\} \text{ is SOS1}, \quad \forall r \in R \tag{E.59}$$

Constraints for the variables:

$$M_r \in \mathbb{Z}, \quad \forall r \in R \tag{E.60}$$

$$z_{gi,r} \in \{0,1\}, \quad \forall r \in R \tag{E.61}$$

$$z_{wi,r} \in \{0,1\}, \quad \forall r \in R \tag{E.62}$$

$$N_{op,r}^t \in \mathbb{Z}, \quad \forall r \in R \quad \text{and} \quad \forall t \in T \tag{E.63}$$

$$N_{gi,r}^t \in \mathbb{Z}, \quad \forall r \in R \quad \text{and} \quad \forall t \in T \tag{E.64}$$

$$N_{wi,r}^t \in \mathbb{Z}, \quad \forall r \in R \quad \text{and} \quad \forall t \in T \tag{E.65}$$

$$N_{wt,r}^t \in \mathbb{Z}, \quad \forall r \in R \quad \text{and} \quad \forall t \in T \tag{E.66}$$

$$N_{op,f}^t \in \mathbb{Z}, \quad \forall t \in T \tag{E.67}$$

$$N_{gi,f}^t \in \mathbb{Z}, \quad \forall t \in T \tag{E.68}$$

$$N_{wi,f}^t \in \mathbb{Z}, \quad \forall t \in T \tag{E.69}$$

$$N_{wt,f}^t \in \mathbb{Z}, \quad \forall t \in T \tag{E.70}$$

$$\text{All variables} \geq 0 \tag{E.71}$$

Appendix F. MILP Formulation of the Optimization Problem to Maximize NPV

Objective function:

$$\text{maximize} \quad NPV \tag{F.1}$$

In this formulation, we use all constraints involved in the previous optimization model (one provided in Appendix E), except Eq. (E.2). Some additional constraints are included to compute NPV.

Constraint to calculate EXPEX:

$$P_{v,ex} = \sum_{t\in\{-3,-2,\ldots,0\}} \frac{A_t}{(1+d)^{(t+3)}} \tag{F.2}$$

Constraints to calculate DRILLEX:

$$P_{v,dx}^{pre-drilled} = \frac{B\cdot N_{wt,f}^1}{(1+d)^3} \tag{F.3}$$

$$P_{v,dx}^t = \frac{B\cdot\left(N_{wt,f}^{t+1} - N_{wt,f}^t\right)}{(1+d)^{(t+3)}}, \quad \forall t \in \{1,2,\ldots,n_t-1\} \tag{F.4}$$

Constraint to calculate ABEX:

$$P_{v,ax} = \left(\sum_{t\in\{-3,-2,\ldots,0\}} \frac{C_t}{(1+d)^{(t+3)}}\right) + D_1\cdot N_{op,f}^{n_t} + D_2\cdot\left(N_{gi,f}^{n_t} + N_{wi,f}^{n_t}\right) \tag{F.5}$$

Constraints to calculate CAPEX-SUB:

$$P_{v,sx} = \sum_{t\in\{-3,-2,\ldots,0\}} \frac{E_1\cdot N_{st,f} + E_2\cdot N_{xt,f}}{4\cdot(1+d)^{(t+3)}} \tag{F.6}$$

$$N_{st,f} = \sum_{r \in R} N_{st,r} \tag{F.7}$$

$$N_{st,r} \geq \frac{N_{op,r}^{n_t}}{4}, \quad \forall r \in R \tag{F.8}$$

$$N_{xt,f} = N_{gi,f}^{n_t} + N_{wi,f}^{n_t} \tag{F.9}$$

Constraints to calculate CAPEX-TOP:

$$F_{v,tx} = G_1 \cdot q_o^{capacity} + G_2 \cdot q_g^{capacity} + G_3 \cdot q_w^{capacity} \tag{F.10}$$

$$P_{v,tx} = \sum_{t \in \{-3,-2,\ldots,0\}} \frac{F_{v,tx}}{4 \cdot (1+d)^{(t+3)}} \tag{F.11}$$

$$q_o^{capacity} \geq q_{o,f}^t, \quad \forall t \in \{2, \ldots, n_t\} \tag{F.12}$$

$$q_g^{capacity} \geq q_{g,f}^t, \quad \forall t \in \{2, \ldots, n_t\} \tag{F.13}$$

$$q_w^{capacity} \geq q_{w,f}^t, \quad \forall t \in \{2, \ldots, n_t\} \tag{F.14}$$

Constraints to calculate OPEX:

$$F_{v,ox}^t = H_1 + H_2 \cdot N_{op,f}^{t-1} + H_3 \cdot q_{o,f}^t + H_4 \cdot q_{g,f}^t + H_5 \cdot q_{w,f}^t, \quad \forall t \in \{2, \ldots, n_t\} \tag{F.15}$$

$$P_{v,ox}^t = \frac{F_{v,ox}^t}{(1+d)^{(t+3)}}, \quad \forall t \in \{2, \ldots, n_t\} \tag{F.16}$$

Constraint to calculate revenue:

$$P_{v,re}^t = \frac{P_o \cdot X_r \cdot X_v \cdot \left(N_{p,f}^t - N_{p,f}^{t-1}\right)}{(1+d)^{(t+3)}}, \quad \forall t \in \{2, \ldots, n_t\} \tag{F.17}$$

Constraints to calculate NPV:

$$P_{v,pp} = P_{v,ex} + P_{v,dx}^{pre-drilled} + P_{v,ax} + P_{v,sx} + P_{v,tx} \tag{F.18}$$

$$D_{cf}^1 = -P_{v,dx}^1 \tag{F.19}$$

$$D_{cf}^t = P_{v,re}^t - P_{v,ox}^t - P_{v,dx}^t, \quad \forall t \in \{2, 3, \ldots, n_t - 1\} \tag{F.20}$$

$$D_{cf}^{n_t} = P_{v,re}^{n_t} - P_{v,ox}^{n_t} \tag{F.21}$$

$$NPV = -P_{v,pp} + \sum_{t \in T} D_{cf}^t \tag{F.22}$$

Constraints for the variables:

$$N_{st,r} \in \mathbb{Z}, \quad \forall r \in R \tag{F.23}$$

$$N_{st,f} \in \mathbb{Z} \tag{F.24}$$

$$N_{xt,f} \in \mathbb{Z} \tag{F.25}$$

All variables except D_{cf}^t and $NPV \geq 0$ (F.26)

Appendix G. Extended Optimization Results

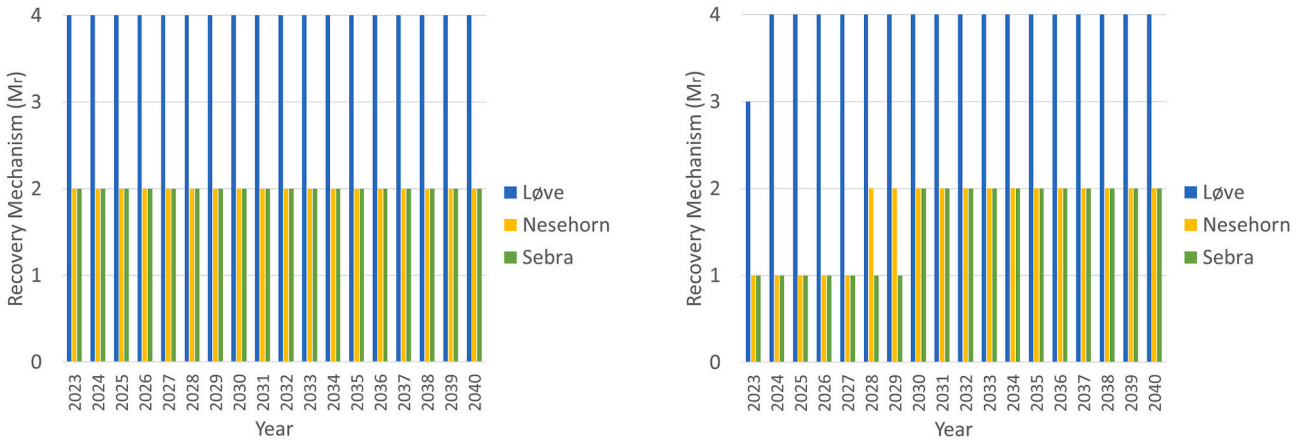

(a) CASE-1 (b) REF-CASE-1

Fig. G.1. Comparison of optimization results between CASE-1 and REF-CASE-1: recovery mechanism. Description on the value of M_r: 1 = natural depletion, 2 = water injection, 3 = gas injection, 4 = water & gas injection.

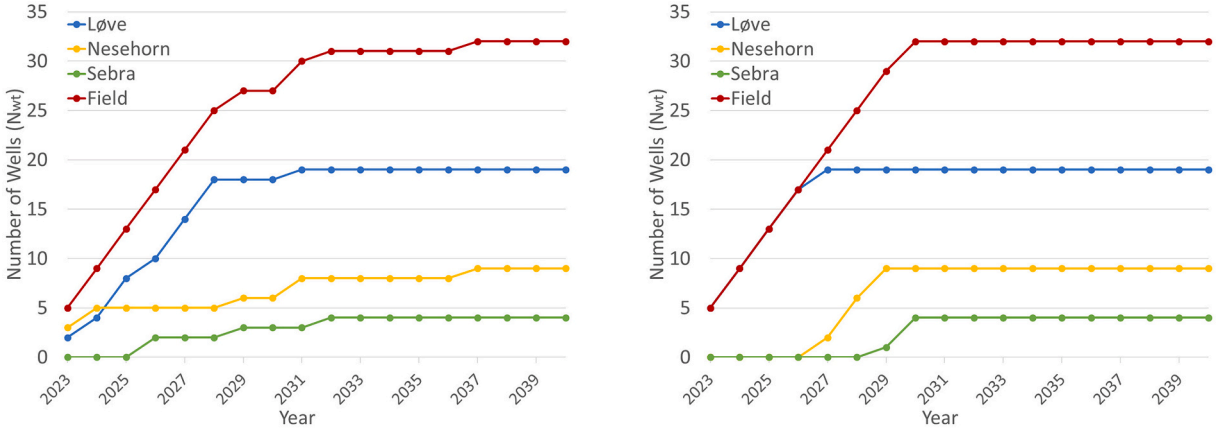

(a) CASE-1 (b) REF-CASE-1

Fig. G.2. Comparison of optimization results between CASE-1 and REF-CASE-1: drilling schedule

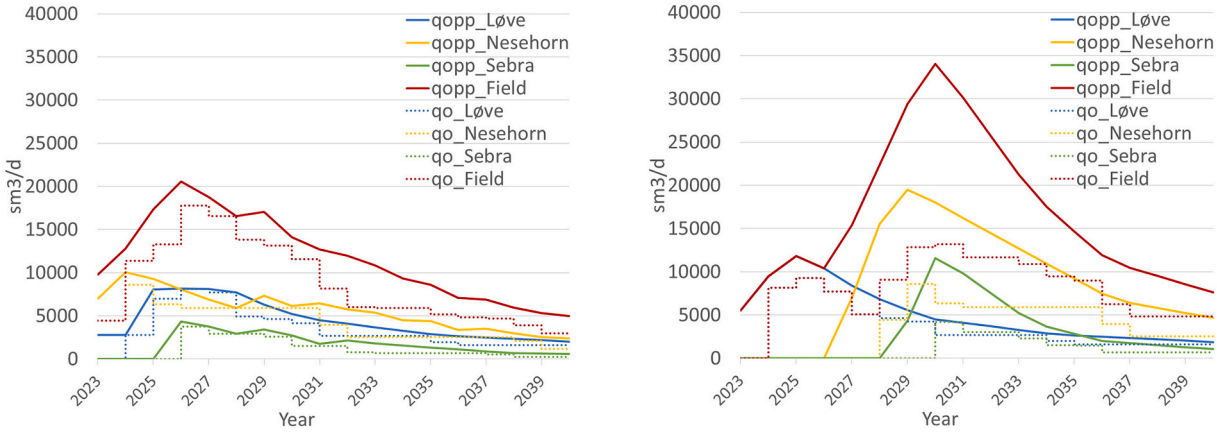

(a) CASE-1 (b) REF-CASE-1

Fig. G.3. Comparison of optimization results between CASE-1 and REF-CASE-1: oil production rate and potential

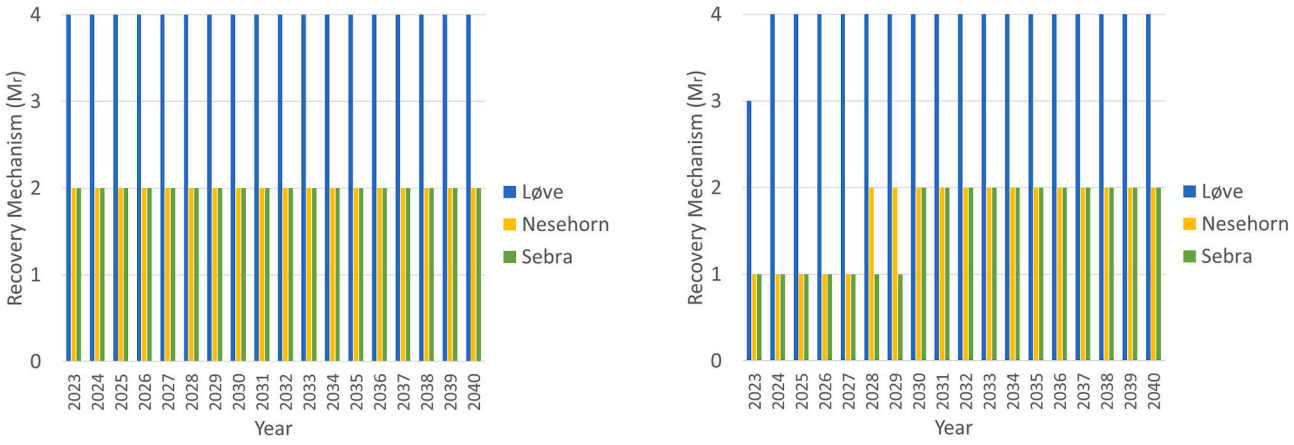

(a) CASE-2 (b) REF-CASE-2

Fig. G.4. Comparison of optimization results between CASE-2 and REF-CASE-2: recovery mechanism. Description on the value of M_r: 1 = natural depletion, 2 = water injection, 3 = gas injection, 4 = water & gas injection.

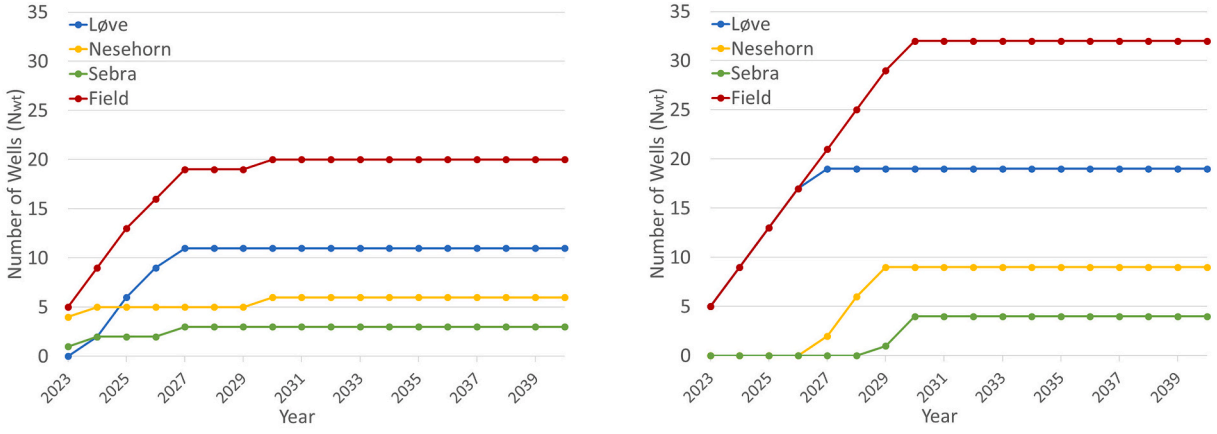

(a) CASE-2 (b) REF-CASE-2

Fig. G.5. Comparison of optimization results between CASE-2 and REF-CASE-2: drilling schedule

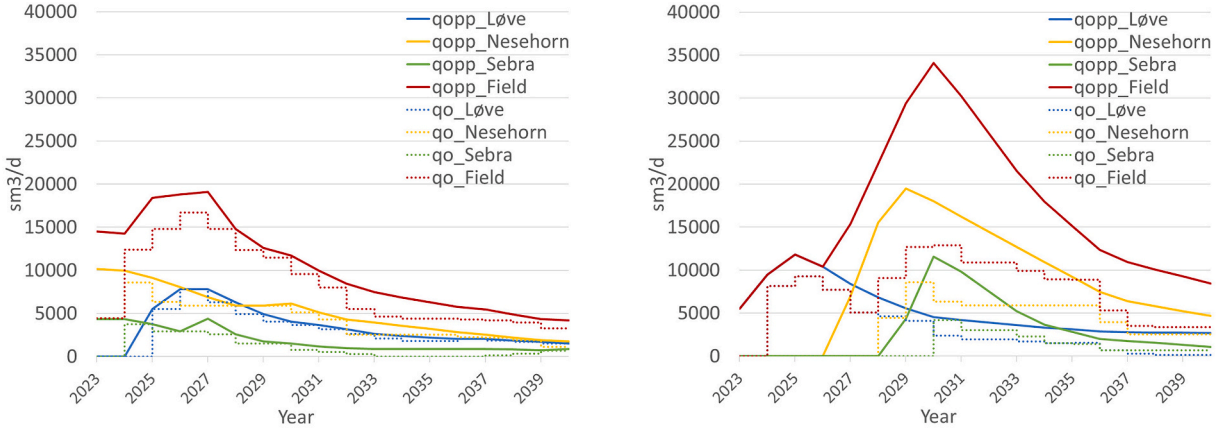

(a) CASE-2 (b) REF-CASE-2

Fig. G.6. Comparison of optimization results between CASE-2 and REF-CASE-2: oil production rate and potential

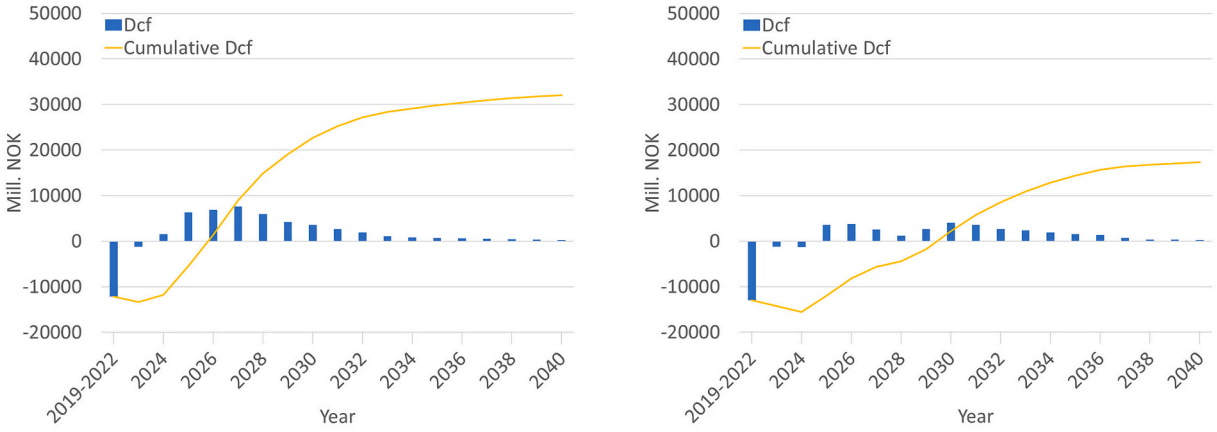

(a) CASE-2 (b) REF-CASE-2

Fig. G.7. Comparison of optimization results between CASE-2 and REF-CASE-2: discounted cash flow and its cumulative

Appendix H. Source Code Availability

The source codes of the optimization models are available under GNU GPL v3 (2007) license on GitHub.[1]

References

Alexander Hall, N., Delille, S., 2011. Cost estimation challenges and uncertainties confronting oil and gas companies. In: 2011 AACE International Transactions. AACE International. https://www.dace.nl/download/?id=17693540. (Accessed 31 January 2020).

AMPL, 2020. AMPL: Streamlined Modeling for Real Optimization. https://ampl.com/. (Accessed 31 January 2020).

Angga, I.G.A.G., 2019. Automated Decision Support Methodologies for Field Development: the Safari Field Case. Master's thesis. Norwegian University of Science and Technology. http://hdl.handle.net/11250/2625934.

Bellout, M.C., Echeverría Ciaurri, D., Durlofsky, L.J., Foss, B., Kleppe, J., 2012. Joint optimization of oil well placement and controls. Comput. Geosci. 16, 1061–1079. https://doi.org/10.1007/s10596-012-9303-5.

Codas, A., Campos, S., Camponogara, E., Gunnerud, V., Sunjerga, S., 2012. Integrated production optimization of oil fields with pressure and routing constraints: the Urucu field. Comput. Chem. Eng. 46, 178–189. https://doi.org/10.1016/j.compchemeng.2012.06.016.

Crowder, H., Johnson, E.L., Padberg, M., 1983. Solving large-scale zero-one linear programming problems. Oper. Res. 31, 803–834. https://doi.org/10.1287/opre.31.5.803.

Dantzig, G.B., 1951. Maximization of a linear functions in variables subject to linear inequalities. In: Koopmans, T. (Ed.), Activity Analysis of Production and Allocation. Wiley & Chapman-Hall, pp. 339–347.

Dantzig, G.B., 1963. Linear Programming and Extensions. Princeton University Press. https://doi.org/10.7249/R366.

Dümbgen, L., Riedwyl, H., 2007. On fences and asymmetry in box-and-whiskers plots. Am. Statistician 61, 356–359. https://doi.org/10.1198/000313007X247058.

GNU GPL v3, 2007. GNU General Public License. https://www.gnu.org/licenses/gpl-3.0.html. (Accessed 31 January 2020).

González, D., Stanko, M., Hoffmann, A., 2019. Decision support method for early-phase design of offshore hydrocarbon fields using model-based optimization. Journal of Petroleum Exploration and Production Technology. https://doi.org/10.1007/s13202-019-00817-z.

Grötschel, M., Holland, O., 1991. Solution of large-scale symmetric travelling salesman problems. Math. Program. 51, 141–202. https://doi.org/10.1007/BF01586932.

Gurobi Optimization, 2020. Gurobi Optimizer. https://www.gurobi.com/products/gurobi-optimizer/. (Accessed 31 January 2020).

Haldorsen, H.H., 1996. Choosing between rocks, hard places and a lot more: the economic interface. In: Dore, A., Sinding-Larsen, R. (Eds.), Quantification and Prediction of Hydrocarbon Resources. Elsevier, pp. 291–312. https://doi.org/10.1016/S0928-8937(07)80025-7.

Hamann, B., Chen, J.L., 1994. Data point selection for piecewise linear curve approximation. Comput. Aided Geomet. Des. 11, 289–301. https://doi.org/10.1016/0167-8396(94)90004-3.

Hoffman, K.L., Padberg, M., 1991. Improving LP-representations of zero-one linear programs for branch-and-cut. ORSA J. Comput. 3, 121–134. https://doi.org/10.1287/ijoc.3.2.121.

Hoffmann, A., 2014. Application of Piecewise Linear Models to Short-Term Oil Production Optimization. Master's thesis. Norwegian University of Science and Technology.

Hoffmann, A., Stanko, M., 2017. Short-term model-based production optimization of a surface production network with electric submersible pumps using piecewise-linear functions. J. Petrol. Sci. Eng. 158, 570–584. https://doi.org/10.1016/j.petrol.2017.08.063.

Hoffmann, A., Stanko, M., González, D., 2019. Optimized production profile using a coupled reservoir-network model. Journal of Petroleum Exploration and Production Technology 9, 2123–2137. https://doi.org/10.1007/s13202-019-0613-1.

IBM, 2020. IBM CPLEX Optimizer. https://www.ibm.com/analytics/cplex-optimizer. (Accessed 31 January 2020).

Jahn, F., Cook, M., Graham, M., 2008. The field life cycle. In: Hydrocarbon Exploration and Production, 2 ed. Elsevier, pp. 1–7 (chapter 1).

Jonsbråten, T.W., 1998. Oil field optimization under price uncertainty. J. Oper. Res. Soc. 49, 811–818. https://doi.org/10.1057/palgrave.jors.2600562.

Litvak, M.L., Angert, P.F., 2009. Field development optimization applied to giant oil fields. In: SPE Reservoir Simulation Symposium, the Woodlands, Texas, USA, 2-4 February. Society of Petroleum Engineers. https://doi.org/10.2118/118840-MS.

Litvak, M.L., Gane, B.R., Williams, G., Mansfield, M., Angert, P.F., Macdonald, C.J., McMurray, L.S., Skinner, R.C., Walker, G.J., 2007. Field development optimization technology. In: SPE Reservoir Simulation Symposium, Houston, Texas, USA, 26-28 February. Society of Petroleum Engineers. https://doi.org/10.2118/106426-MS.

Litvak, M.L., Onwunalu, J.E., Baxter, J., 2011. Field development optimization with subsurface uncertainties. In: SPE Annual Technical Conference and Exhibition, Denver, Colorado, USA, 30 October-2 November. Society of Petroleum Engineers. https://doi.org/10.2118/146512-MS.

McNamee, P., Celona, J., 2008. Decision Analysis for the Professional, 4 ed. SmartOrg, Inc https://smartorg.com/wp-content/uploads/2011/08/Decision-Analysis-for-the-Professional.pdf. (Accessed 31 January 2020).

Nazarian, B., 2002. Integrated Field Modeling. Ph.D. thesis. Norwegian University of Science and Technology. https://pdfs.semanticscholar.org/f519/6deab179457ccc4b7df5c420822069b9f381.pdf?_ga=2.241207938.1025787651.1577989669-1837184426.1577989669. (Accessed 31 January 2020).

NPD, 2020. NPD FactMaps. https://factmaps.npd.no/factmaps/3_0/. (Accessed 31 January 2020).

Padberg, M., Rinaldi, G., 1991. A branch-and-cut algorithm for the resolution of large-scale symmetric traveling salesman problems. SIAM Rev. 33, 60–100. https://doi.org/10.1137/1033004.

Petroleum Experts, 2020. IPM Suite. https://www.petex.com/products/ipm-suite/. (Accessed 31 January 2020).

Silva, T.L., Camponogara, E., 2014. A computational analysis of multidimensional piecewise-linear models with applications to oil production optimization. Eur. J. Oper. Res. 232, 630–642. https://doi.org/10.1016/j.ejor.2013.07.040.

[1] https://github.com/stankome/EarlyFieldDesign-Angga.

Silva, T.L., Codas, A., Stanko, M., Camponogara, E., Foss, B., 2019. Network-constrained production optimization by means of multiple shooting. SPE Reservoir Eval. Eng. 22 https://doi.org/10.2118/194504-PA.

Simonov, M., Shubin, A., Penigin, A., Perets, D., Belonogov, E., Margarit, A., 2019. Optimization of oil field development using a surrogate model: case of miscible gas injection. In: SPE Reservoir Characterisation and Simulation Conference and Exhibition, Abu Dhabi, UAE, 17-19 September. Society of Petroleum Engineers. https://doi.org/10.2118/196639-MS.

Stanko, M., 2020. Observations on and use of curves of current dimensionless potential versus recovery factor calculated from models of hydrocarbon production systems. J. Petrol. Sci. Eng. https://doi.org/10.1016/j.petrol.2020.108014.

The Ministry of Petroleum and Energy and the Ministry of Labour and Social Affairs, 2018. Guidelines for Plan for Development and Operation of a Petroleum Deposit (PDO) and Plan for Installation and Operation of Facilities for Transport and Utilisation of Petroleum (PIO). https://www.npd.no/globalassets/1-npd/regelverk/forskrifter/en/pdo-and-pio.pdf. (Accessed 31 January 2020).

Tupac, Y.J., Almeida, L.F., Vellasco, M.M.B.R., 2007. Evolutionary optimization of oil field development. In: Digital Energy Conference and Exhibition, Houston, Texas, USA, 11-12 April. Society of Petroleum Engineers. https://doi.org/10.2118/107552-MS.

Volz, R.F., Burn, K., Litvak, M.L., Thakur, S.C., Skvortsov, S., 2008. Field development optimization of eastern Siberian giant oil field development under uncertainty. In: SPE Russian Oil and Gas Technical Conference and Exhibition, Moscow, Russia, 28-30 October. Society of Petroleum Engineers. https://doi.org/10.2118/116831-MS.